MODEL TESTS TO PREDICT THE SEAWORTHINESS OF SEAPLANE HULLS

by
E. F. Schulz

Civil Engineering Section
Colorado A and M College
Fort Collins, Colorado

prepared for

BUREAU OF AERONAUTICS
Navy Department
under Contract No. NOas 54 - 908 c
through the
Colorado A and M Research Foundation

January 1957

CER No 57 EFS 1

CONTENTS

ABSTRACT

The seaworthiness of two model seaplane hulls having length-to-beam ratios of 8 and 12 was estimated by observing the motions of heaving, pitching and rolling while towing the models at various speeds, model loadings and at various headings to a simple wave front. All the experiments were made in the pre-hump speed range.

The important parameters determining the motions of a seaplane operating in this speed range were found to be the effective tuning ratio, the relative wave-hull length ratio and the damping ratio.

Increasing the hull length-beam ratio from 8 to 12 results in improved seaworthiness at the speeds tested. Shifting of the relative wave-hull length ratio to less critical values can be obtained by changing the angle of heading from "into the waves" to "parallel to the wave crests". Shifting of the tuning ratio to less critical values can be obtained by changing the heading from "into the waves" to "with the waves".

NOTATION AND DEFINITIONS

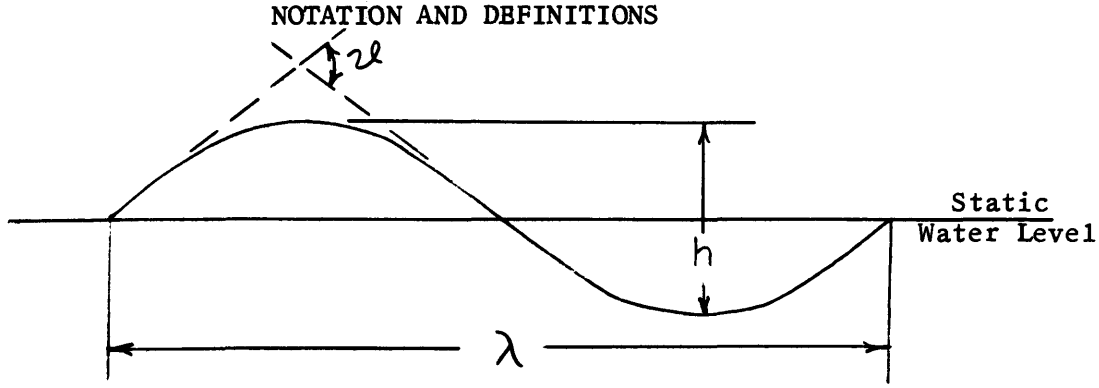

Symbol	Units	Definition
λ	feet	Wave length
h	feet	Wave height
$\omega = 2\pi f$	-	Circular wave frequency
f	cps	Wave frequency
$T = 1/f$	seconds	Wave period
c	fps	Wave celerity
2ℓ	degrees	Wave slope
w	lb/ft^3	Unit weight of water

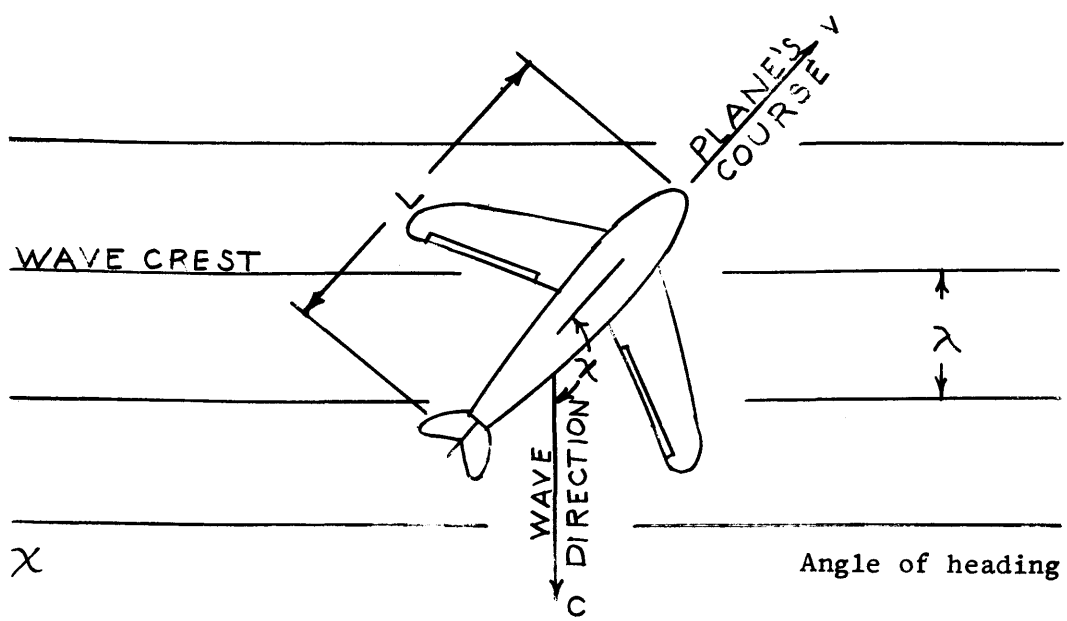

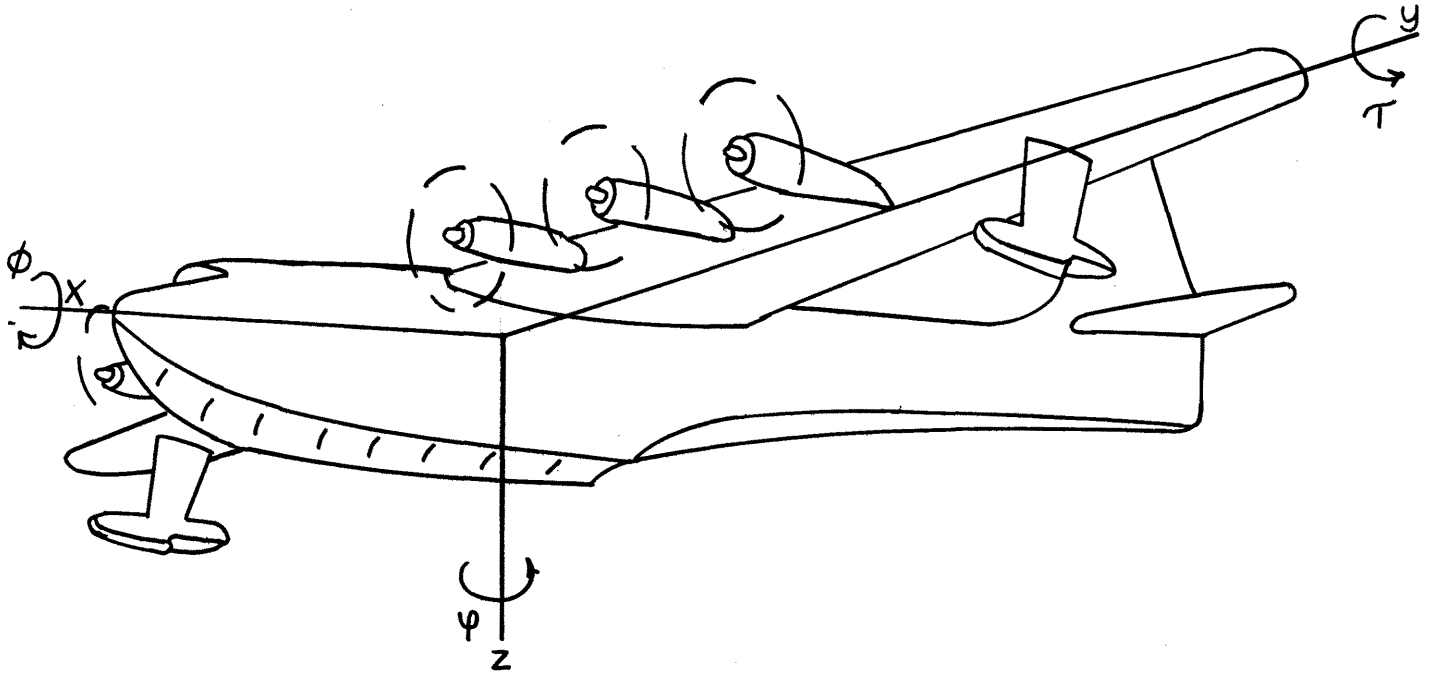

Symbol	Units	Definition
L	feet	Length of hull
Δ	pounds	Load of hull on water
b	feet	Maximum beam of hull
s	feet	Span between wing tip floats; also refers to motion
v	fps	Average magnitude of speed of model
ΔZ	feet	Heave or translation along z-axis
$\Delta\tau$	degrees	Maximum change in trim angle
$\Delta\phi$	degrees	Maximum change in roll angle
A_s	-	Amplitude parameter for motion, s
A_τ	-	Trim parameter factor
A_z	-	Heave parameter factor
A_ϕ	-	Roll parameter factor
$\wedge$	-	Tuning ratio
C_v	-	Speed coefficient -- $\frac{v}{\sqrt{gb}}$
C_Δ	-	Load coefficient --------- $\frac{\Delta}{wb^3}$

I. INTRODUCTION

The term "seaworthiness", as applied to aircraft, has been defined as the ability of a seaplane to remain operational under conditions found in heavy seas, i.e. the seaplane must be able to land and take off as well as remain afloat without damage from the waves.

Until the institution of the present study, the seaworthiness of a seaplane had been predicted from tests of a model towed head-on into a train of uniform waves. Predictions made from model tests were then correlated with observations made during flight tests of the prototype aircraft.

Conditions in nature, however, are frequently such that it is impossible or undesirable for a seaplane to take off and land head-on into a train of uniform waves. Quite often the course of the aircraft is at some angle to the wave train.

Because previous model tests of seaplane seaworthiness have only remotely resembled conditions found in nature, the strong need for developing more realistic testing techniques has been recognized. The present study was initiated, therefore, to test a model in a simple wave train at angles other than head-on.

It is recognized that in the natural condition there probably would be several wave trains present coming at different angles and consisting of different periods and amplitudes -- the result being a confused sea. Because the problem of generating a reproducible confused sea in the laboratory is very complicated, the present study was limited

to a simplified case. A basic understanding of the relationships involved could be gained most rapidly by considering the simple sea on oblique headings first. It was hoped that suitable techniques could be developed whereby the way would be opened to consider more complicated conditions.

The tests were conducted by towing two different models at various angles with respect to a rectilinear sea of discrete frequency, The purposes of the experiments were two fold:

1. To develop testing techniques, and
2. To determine if the techniques would differentiate between the behavior of the two models.

The work described in this report was conducted for the Bureau of Aeronautics, Navy Department under Contracts No as 52-1077c and NO as 54-908c.

II. DESCRIPTION OF EQUIPMENT

The experimental apparatus was previously described in (5)[1].

Models

The two models were previously employed during a systematic investigation of the effect of increasing the length-to-beam ratio of a series of seaplane hull forms. Hull lines for the two models are shown in Fig. 1 and 2. The hulls had a length-to-beam ratio of 8 and 12. An aluminum channel section was fitted to the hull to support the wing-tip floats. The span between tip floats was arbitrarily made equal to the hull length. The tip float lines were based on the design of the XP5Y-1 floats. The length of the floats was arbitrarily made one-seventh of the length of the hull. Fig. 3 is a photograph showing the two models in the testing configuration.

The floats were given a 3° nose-up trim relative to the forebody keel at the step. The float draft was adjusted so that the hull could heel over 3° to either side before the respective float was entirely effective. The model particulars are listed in Table 1.

[1] Figures in parentheses refer to the references listed at the end of this report.

III. LABORATORY PROCEDURE AND EQUIPMENT

The variables considered important to the motion of seaplanes were, (a) angle of heading of seaplane relative to direction of wave travel, χ ; (b) model speed, C_V , and (c) wave length, λ . A detailed list of all variables and their range of variation considered in this study is given in Table 2. During the 1953 experiments, model headings of 90°, 120°, 135°, 150° and 180° were used. In 1954 the models were tested on headings of 0°, 45°, 90°, 135° and 180°.

Model Loading

The planform area and gross weight of the two models were the same, hence the load coefficients $(\frac{\Delta}{wb^3})$ of the models were different because the beam loading differed.

Since aerodynamic lift was not "modelled" in the tests, the hulls were artificially "unloaded" as the testing speeds were increased by removing ballast.

During the 1953 tests the models were towed at two values of gross weight through the entire speed range. During the 1954 tests the models were towed at the different speeds at loadings determined from a parabolic unloading curve. Two unloading curves enveloping the range of practical seaplane operations were used. The unloading curves varied between $2.0 < C_{\Delta_o} < 3.0$ and take off speed coefficients of $6.0 < C_{V_{TO}} < 8.0$.

Care was taken when removing the ballast to maintain the center of gravity at the specified location. The location of the center of

gravity was determined by suspending the model from a single point at the bow and at one wing tip. The moment of inertia was determined by suspending the model as a torsional pendulum from a 20-ft length of steel wire which had been calibrated. The values of the moment of inertia are tabulated in Table 3.

Towing Equipment

The model was towed with a bridle. The towing thrust was applied by the bridle attached to the model along the lateral axis through the center of gravity; hence the towing did not influence the pitching moment of the models. The towing bridle is shown attached to the nearest model in Fig. 3. The towing motor and related equipment are described in (5).

Wave Properties

The wave profile was sampled by a single resistance probe. The wave probe was cleaned and calibrated daily. The wave length was computed from the deep-water wave period using the equation

$$\lambda = \frac{gT^2}{2\pi} \quad .$$

Tabulated values of the wave properties used may be found in (9).

Movie Film Records

For the needs of this report the model motion data were taken from the front and side view movies. The wave period, wave height, and model speed were obtained from the oscillograph records.

Several methods of reducing the measurements from the movie film were tried. The movies were projected on a sheet of white paper with a standard 16-mm movie projector which had been modified so that it could be stopped at any frame without damage to the film. The attitude of the model relative to a horizontal datum and the position of the center of gravity relative to a horizontal datum were traced on the paper. These tracings were then processed using protractors and scales to determine the following:

1. Change in trim angle, $\Delta \tau$,
2. Change in heave, Δz, and
3. Change in angle of roll, $\Delta \phi$.

Convectron Tube Records

As suggested in (5), it was planned to use the convectron tubes to measure angles of trim and roll. Movies were taken from the front and side during all tests to facilitate the dynamic calibration of the convectron tubes. Figs. 4 through 8 show comparisons of the trim and roll measurements made by the convectron tubes with those taken from the movie data. Examination of these graphs leads to the conclusion that the convectron tubes do not satisfactorily measure the angles of trim and roll of a model seaplane. This is attributed to the acceleration sensitive features of the convectron tubes.

It is possible to use the convectron data if the longitudinal and lateral accelerations could be measured and these measurements deducted from the convectron tube indication. The convectron data could

also be analysed if a particular angle of trim or roll were always associated with the same value of acceleration. Unfortunately, both phase and amplitude relationships between the attitude and accelerations evidently change with angle of heading, wave period, and speed. In some cases where the associated accelerations are small, i.e. roll on Fig. 4, there is a fair agreement between the movie and the convectron data. On the other hand the accelerations may cause convectron readings which exceed the reading due to the angle, i.e. trim on Fig. 4.

Limits of Precision

The measurements made during these experiments are believed to be accurate within the following limits:

Model Speed	± 0.05 fps
Angle of trim or roll	± 0.5 degree
Heave	± 0.04 ft
Wave height	± 0.02 ft
Wave period	± 0.1 sec
Time from oscillographic records	± 0.01 sec
Time from movie records	± 0.02 sec

IV. PRESENTATION AND ANALYSIS OF DATA

These data were analysed on the basis of the theoretical work on ship motions outlined in (6), (7) and (10). These theoretical studies are summarized in (8).

In the case of a ship moving in a regular seaway, the motions of the ship are the result of the waves which generate the exciting force. The resultant reactions of the ship are classified as the inertial forces, the damping forces, and the restoring forces. A general equation of motion as shown in (8) is as follows:

$$Q \frac{d^2 s}{dt^2} + \ldots N \frac{ds}{dt} + \ldots \quad Rs = F(s, t) , \tag{1}$$

where s represents any translational or rotational oscillatory motion of the seaplane, and

$+ \ldots$ represents coupling terms.

The three translational motions and the three rotational motions can all be reduced to pitching, heaving and rolling by assuming a number of linearizations. These three simultaneous equations result:

$$z = r_m A_z \cos(\omega_e t - \epsilon_z) , \tag{2}$$

$$\tau = r_m A_\tau \cos(\omega_e t - \epsilon_\tau) , \tag{3}$$

$$\phi = r_m A_\phi \cos(\omega_e t - \epsilon_\phi) , \tag{4}$$

where r_m is the applicable wave function,

A_s is the amplitude parameter for that particular motion, s ,

ω_e is the frequency of encounter of the waves,

ϵ_s is the total applicable phase shift for that particular motion, s .

The applicable wave function, r_m , for a sinusoidal wave is defined as the total wave height, h , for heave, and the change in wave slope, ϑ , for trim and roll as illustrated below:

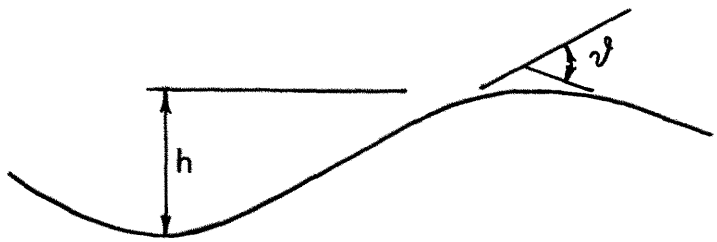

The amplitude parameter is a dimensionless parameter which expresses the magnitude of the model motion relative to the size of the wave as follows:

for heaving $A_z = \Delta z/h$, (5)

for pitching $A_\tau = \Delta\tau/\vartheta$, (6)

for rolling $A_\phi = \Delta\phi/\vartheta$. (7)

The frequency of encounter, ω_e , is the term which defines the relative frequency with which the seaplane encounters the waves and is given by the equation:

$$\omega_e = (1 - \alpha) = \omega\left(1 - \frac{v \cos\chi}{c}\right) , \quad (8)$$

where ω is the circular wave frequency, and

α is the ratio of seaplane speed in the direction of wave travel to the wave celerity.

When the seaplane has an appreciable component of velocity in the same direction as the wave travel, or the seaplane speed is great enough in the direction of wave travel, so that $\alpha \geq 1$, then the frequency of encounter computed by Eq 8 becomes negative. When $\alpha \geq 1$, the seaplane is encountering the waves in the inverse order from which they were generated.

The total phase shift, ϵ_s, is the sum of two elements. One element is a result of inertial effects and is commonly found in periodic or harmonic motion. The second element is the effect of changes in the velocity field around the hull due to its motion and to the "added mass" or entrained water.

As shown in (8) the amplitude parameters, A_s, are a function of the effective tuning ratio for any particular motion, given in parameters of the relative wave length. The effective tuning ratio is expressed by:

$$\Lambda_e = \Lambda_s (1 - \alpha) , \qquad (9)$$

where Λ_s is the tuning ration for the motion, and

α is the relative seaplane speed from Eq. 8.

The tuning ratio is the ratio of the wave frequency and the natural undamped frequency of the seaplane in that particular degree of freedom concerned.

$$\Lambda_s = \frac{\omega}{\nu_s} \tag{10}$$

where ω is the wave frequency, and

ν_s is the natural undamped frequency.

The effects of the variable heading relative to the wave travel are accounted for by multiplying by the "encounter factor", $1 - \alpha$. The effective tuning ratio is defined as:

$$\Lambda_e = \frac{\omega_e}{\nu_s} = \frac{T_n}{T_e} \quad , \tag{11}$$

where T_n is the natural period of the hull in seconds, and

T_e is the period of encounter in seconds.

The relative wave length mentioned in connection with Eq 9 is defined as the ratio of the hull length and the wave length:

$$\lambda/L \ . \tag{12}$$

Actually, in an oblique sea, the relative wave length is more realistically:

$$\frac{\lambda}{L \cos \chi} \ .$$

However, since the data are separated according to heading, the correction for the obliquity of the wave front is included in the data identified by the various values of λ/L in Figs. 10a through 10e.

Presentation of Data

The experimental data are tabulated in Table 4. Included in this table are the parameters which were used in the analysis. Graphs of the amplitude parameter vs effective tuning ratio are shown in Fig. 9. This graph gives a comparison of the two hulls for the three motions - trim, heave and roll. The amplitude parameter is shown in terms of the relative wave length (λ/L). The envelope of maximum values is shown as a solid line. Mean values of the motion are shown as a broken line.

Polar diagrams illustrating the effect of heading on the amplitude parameter are shown in terms of the relative wave length in Fig. 10. Here again the data for the two hulls and the different motions are shown as a comparison graph. The lines drawn here are envelope values and represent probable maximum values of the motion at any particular heading and relative wave length.

The correlations of seaplane motions as expressed by the amplitude parameter and speed coefficient are shown on Fig. 11. The lines drawn are mean values at any particular speed and relative wave length.

Correlations of the amplitude parameters to relative wave length are shown in Fig. 12. These correlations are shown for two speeds - 0 and 13.8 fps. Since the two hulls had different beam widths, the speed coefficients were 3.5 and 3.7 for the $L/b = 12$ hull and the $L/b = 8$ hull respectively. These curves represent mean values of the amplitude parameter.

V. DISCUSSION OF RESULTS

In order to examine the results of these experiments in terms of a real seaway, a brief discussion of the seaway will be introduced.

The Seaway

The properties of ocean waves have been discussed in (4) and (7). The waves present in the ocean are classified into "sea" and "swell". The waves experienced in a storm area generated by the local winds of the storm are called "sea". When the waves travel out of the storm area, they change into "swell".

The salient features of "sea" waves are:

1. Individual waves have sharp angular tops.
2. The waves are short-crested. The crest line is usually only two or three wave lengths long.
3. The waves are relatively steep.
4. Small waves may be added to other larger waves.

Sometimes the individual crests may seem to line up with other crests; at other times the lines of crests seem to intersect at angles of 20° to 30° to each other. The short crested feature is caused by intersecting wave systems.

"Swell" is characterized by these features:

1. Swell waves are low with rounded tops.
2. Waves following one another are nearly of the same height.
3. The crest lines are usually six or seven times the wave length long.

4. Groups of five to eight waves follow each other followed by relative calm of approximately twenty seconds duration.
5. The waves in the group gradually increase in amplitude toward the middle of the group.

There may be some local choppy waves superimposed on a swell. The presence of the swell can be recognized by the relatively long crest lines. The following diagram shows typical records of sea wave records and swell records taken from (4).

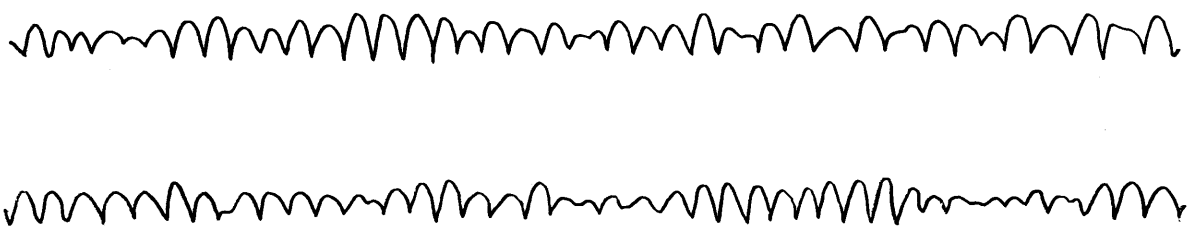

Typical Sea Wave Records

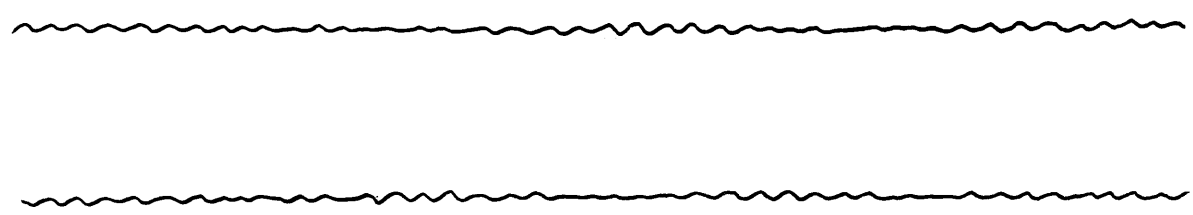

Typical Swell Records

It is shown in (4) and (7) that the ocean waves -- no matter how complex or confused -- are actually composed of the sum of many small sinusoidal wave trains of various heights and wave lengths and travelling in different directions. These elemental waves all obey the classical relationships between celerity, wave length and period as shown in (9).

Operating a seaplane in a "swell" or in a "sea" may call for different techniques. In the presence of a swell, the wind is likely to be calm and the landing or take-off run may be made parallel to the crests and if possible, in the relatively low waves occurring between the "packets" of higher waves.

The landing or take-off run in "sea" waves may well be dictated by the wind conditions present. The steepness and irregularity of the waves are the outstanding features of the sample sea wave records shown previously. Furthermore, it is difficult to predict with a great deal of confidence how high the next wave will be.

Probable Maximum Values

Examination of the various graphs on Fig. 9 indicates that some scatter exists in the data. Because of the scatter, envelope values and mean values have both been shown on these graphs. The envelope lines have been faired through the upper values of the data and are assumed to be probable maximum values of the amplitude parameter. The mean lines are shown as broken lines and present a graphical picture of the relative importance of the scatter of the data. It is advisable to

use the maximum values as indicated by the envelope curves because these extreme values are likely to be associated with large values of acceleration. A large value of A_s means a large amplitude of seaplane motion.

Critical Tuning Ratio

The value of the effective tuning ratio, $\frac{\omega e}{\omega_n}$, at the maximum amplitude parameter is called the critical tuning ratio. In some cases the maximum amplitude parameter is poorly defined and the critical tuning ratio occurs over a range which is referred to as the critical range. The occurrence of a peak value of motion is analogous to resonance in a vibrating system and may also be referred to as synchronism. The critical range should occur when the frequency of encounter is equal to the natural frequency for that motion or when the tuning ratio is unity. The natural frequencies of the hulls were obtained in calm water at zero speed. It has been pointed out in (10) that the orbital velocities of the water particles and the translation of the hull at some speed in the waves cause variations in the exciting force, the damping forces, and the inertial coefficients. These variations cause the critical value to be displaced from the theoretical value of unity and also cause a slight shift with increasing wave length. This is shown in the comparison of heave and roll graphs, Figs. 9c, 9d, 9e, and 9f. The critical tuning ratio for both hulls shows a tendency to increase with increasing wave length for heave, as contrasted with the opposite tendency for roll.

When the amplitude parameter is unity, the total amplitude of motion is equal to the corresponding wave function, i.e. Δ trim = maximum wave slope, Δ roll = maximum wave slope, and Δ heave = total wave height. When the amplitude factors are greater than one, the motion is greater than the wave function. This magnification of the motion is characteristic of synchronism and is limited by the energy dissipative damping forces. If the damping is large, the magnification is small and the peak amplitude parameters are small. Comparing the peak amplitude factors in heave and roll (Figs. 9c and 9d with 9e and 9f) it is evident that damping in heave is greater than in roll.

Trim Parameter

The pitching motion is probably the most important motion since it results in considerable discomfort to the pilot and due to the angular acceleration relatively high load factors on the extreme ends of the seaplane.

Comparison of the envelope curves of the trim parameter for the two hulls indicates that the longer hull generally exhibited smaller trim amplitudes. For the shortest wave length used, the longer hull experienced 30% smaller changes of trim than the short hull. This reduction in trim was only 15% for the two longest wave lengths. The trim parameter showed a critical range between $0.75 < \frac{\omega_e}{\omega_n} < 0.85$. The critical value was well defined for the two longer wave lengths. The critical tuning ratio was independent of relative wave length, λ/L .

Examination of the polar diagrams in Fig. 10 indicates that the greatest pitching amplitudes occur at a heading of 180° with those at 135° being only slightly less. Least pitching occurs at 90° with 45° and 0° next in order of amplitudes.

Comparison of the trim parameters for the two hulls, Fig. 11, shows that for the two longest wave lengths studied, the pitching oscillations increase as the speed increases. When the waves are approximately equal to the hull length, the pitching oscillations are virtually independent of the speed. As the speed increases, the hull passes gradually from a condition where it follows the passing wave contour to a situation where it appears to lose contact with the dropping downslope portion of the wave. At this point the model is in a diving attitude because the afterbody is still in contact with the crest of the wave. At the highest speed tested in the longest wave, the longest hull showed smaller changes in the trim amplitude. Examination of the movies shows that the forebody has opened a large furrow in the crest of the wave and the afterbody has occupied this space before the water can close the gap. The forebody and step areas of the hull were subjected to heavy loads as evidenced by large quantities of milky spray. At lower speeds the spray appears as a clear blister originating near the bow. The blister varies in size as the hull encounters the waves.

The manner in which the pitching amplitudes increase as the wave length is increased is shown in Fig. 12b. Here the trim parameter is shown as a function of relative wave length for the highest speed

tested (approximately 40 percent of getaway speed). This graph shows that both hulls have a critical wave length beyond which the pitching amplitude becomes smaller. This critical wave length occurs when $\lambda/L = 1.9$ for the $L/b = 8$ hull and $\lambda/L = 2.2$ for the $L/b = 12$ hull. As pointed out in (1) and (2), seaplanes experience critical values of maximum trim angle, maximum normal acceleration, and maximum angular acceleration when the wave length is approximately 2.5 times the hull length. Limitations of the wave generator prevented production of waves longer than $\lambda/L = 2.4$.

It is interesting to note that the trim amplitude factor is significantly lower when the effective tuning ratio is zero or negative. These negative values can only occur when the seaplane has a component of velocity in the direction of wave travel greater than the wave celerity. In order to develop the negative ω_e, the seaplane must be travelling with appreciable velocity in the direction of wave travel. In the area where $\alpha > 1$, the differences between the performance of the long and the short hull are less pronounced. In this case, the higher length to beam ratio hull pitches less violently; but it has little advantage from the seaplane motion point-of-view when it travels with the waves.

It is recognized that other factors must be considered in operating and controlling the seaplane on the water. Many times the wind and the sea are running in the same direction. From purely aerodynamic considerations, the pilot would choose landing and taking off into the wind to gain every possible advantage from decreased water speed. Hydrodynamic considerations alone would indicate landing and

taking off or maneuvering should be parallel to the predominant wave crests or with the waves because in this way the maneuver is carried out when far removed from synchronism and the probability of high impact loads are reduced. If the wind and the sea are running in the same direction, this means landing and taking off either crosswind or downwind. This may be inadvisable operationally. The advantages of the longer hull from the pitching point-of-view are clearly evident in those cases where the take-off run must be made into the wind and into the waves.

A limitation of the model data should be pointed out here. The models are not equipped with an empennage. Undoubtedly there would have been some aerodymamic damping of the pitching motion of the seaplane due to the horizontal tail surfaces.

Heave Parameter

Heave herein refers to the vertical translation of the hull caused by the oscillatory motion of the waves. The vertical translation of a seaplane in waves is sometimes referred to as rise. (1), (2) and (3). Naval architects refer to this translation as heave. Use of the word "rise" implies importance of vertical motion due to hydrodynamic lift on the planing hull. Since these hulls were tested at relatively low speed as predominately displacement hulls, the word heave is used in connection with this discussion.

The probable maximum and the mean values of the heave amplitude parameter are shown in Fig. 9c and 9d. Comparison of the heave amplitude parameters for the two hulls indicates that the shorter hull

experienced up to 28 percent larger heaving amplitudes than the $L/b = 12$ hull, except for the longest wave length used, where the longer hull showed about 12 percent higher heaving amplitudes. This can be explained by referring to Fig. 12d. The longest wave used was approximately twice the length of the longer hull whereas this same wave was 2.4 times the length of the shorter hull. Therefore, the short hull was past its critical wave length in the longest waves used. On the other hand, the longer hull appears to have been near its critical wave length.

The critical tuning ratio occurs between $0.50 < \frac{\omega_e}{\omega_n} 0.85$. Examination of the envelope curves on these graphs shows a consistent shifting of the critical tuning ratio to the right as the wave length increases. This shifting is probably caused by variation of the natural frequency of the hull in heave, ω_{n_z}. The virtual mass of the heaving seaplane is affected by the vertical velocity of the water particles, hence the shift in critical tuning ratio when the effective wave length, λ/L, is changed.

Comparison of the polar diagrams, Figs. 10c and 10d, shows that the least desirable heading as far as heaving is concerned is either the 180° (running into waves) or the 135° heading. Here the longer hull again shows different characteristics than the shorter hull. The short hull $(L/b = 8)$ experienced the largest heaving amplitude on the 180° heading (2.1) followed by 135° (1.75), 45° (1.3), 90° (1.1) and 0° (1.0)[1]. The long hull $(L/b = 12)$ experienced the greatest heaving on the 135° heading (1.8) followed by 90° (1.65), 0° (1.12),

[1] Figures in parentheses here refer to the maximum heave parameter for the specified heading.

45^0 (0.98) and 180^0 (0.95) . The longer hull had 10 percent higher beam loading which caused greater chine immersion than the shorter hull experienced. This probably accounts for the smaller heaving amplitude of the long hull.

Comparison of Figs. 11c and 11d indicates that the heave parameter for the long hull shows little variation as the speed was increased from zero to approximately 40 percent getaway speed. The short hull on the other hand, showed some trends toward higher heave parameters for this same increase in speed, particularly for the $\lambda/L = 2.2$ wave. This is probably explained by the fact that this wave length is the critical wave length. Figs. 12c and 12d show the heave parameter as a function of relative wave length for two speed conditions. For the zero-speed both hulls show a gradual increase in heaving amplitude as the wave length is increased from 0.8 to 2.4 times the hull length. For the highest speed used in these tests, the heave parameter has a critical value at $\lambda/L = 2.2$ for the short hull $(L/b = 8)$. Results of the tests on the long hull also indicate that in the case of the heaving motion, the critical relative wave length was greater than $\lambda/L = 2.0$.

Testing these models without wings probably caused somewhat larger-than-normal heaving amplitudes.

Roll Parameter

The roll data were handled in a manner similar to that of the other motions. The envelopes of the roll amplitude parameter are shown

in Figs. 9e and 9f and represent the probable maximum rolling amplitudes for the two hulls. The mean lines are again shown as broken lines. The short hull (L/b = 8) experienced from 7 percent to 14 percent greater rolling amplitudes than the long hull, depending on the wave length considered.

The critical tuning ratio occurs between $0.6 < \frac{\omega_e}{\omega_n} < 1.7$. The critical tuning ratio of the roll parameter decreased as the wave length was increased. This is due to the fact that the rolling cycle is largely dominated by the heaving of the wing-tip floats. Since the heaving of the hull is influenced by the vertical wave velocity effects on the vertical mass, the wing-tip floats are subjected to the same type of effects as the hull.

The wing-tip floats were adjusted so that the hull could heel over 3^0 to either side before the floats were effective. The rolling for somewhat less than 6^0 was damped by the viscous effects of the frictional resistance of the wetted hull surfaces and the eddy making losses due to lateral flow past the keel and chine.

Figs. 10e and 10f show that on the 45^0 heading the hulls experienced the largest rolling amplitudes. The least amplitude of roll occurred at the 0^0 heading. Theoretically the hulls should experience no rolling on either the 0^0 or 180^0 headings; however, the placement of the tip floats permitted some rolling and also at times a tendency for the tip floats to bury themselves was observed. When this happened, high amplitudes of roll were noted.

On the 90° heading relatively large submergence of the tip floats caused noticeable deceleration due to the additional heavy drag on the floats. This occurred when the hull settled in the trough of the wave forcing the tip floats under at or near the crests of the waves. As the speed increased the model would rise in the water tending to relieve the forced submergence of the floats.

Examination of Figs. 11e and 11f shows that for the shortest wave length used there is little change in the roll parameter as the speed varies. On the other hand, for the other wave lengths the roll parameters first increase and then decrease after the speeds exceed $C_V = 0.8$. This decrease is related to the manner in which the hull rises with increasing speed, giving the wing-tip floats greater clearance with less chance for a roll oscillation to start.

Figs. 12e and 12f illustrate how the roll parameter varies with relative wave length for the zero-speed and the highest speed tested. When the seaplane is hove-to, the rolling amplitudes increase for both hulls as the wave length increases up to $\lambda/L = 2.4$. This is quite logical in light of the previous discussion on the 90° heading. When the wave length is equal to the span between wing-tip floats as is the case for $\lambda/L = 1.0$, the hull has little opportunity to heel over between wave encounters because of the relatively long time during each encounter that the tip floats are simultaneously submerged. As the heading changes from 90° to 180° or as the wave length increases from $\lambda/L = 1.0$ to 2.5, the seaplane has not only a greater opportunity to

roll but the positive buoyancy of first one and then the other tip float causes the rolling to start. For this reason the wing-tip floats provide a dual, and seemingly opposite, role in the rolling motion:

1. The tip float may actually start the rolling cycle when one wing-tip float encounters the wave before the hull or the other float.
2. The tip float prevents excessive rolling (capsizing) of the hull.

At 40 percent of the getaway speed, the roll parameter appeared much the same as the parameter for pitching and heaving at this speed. The difference between the long and the short hull was slight, and the short hull ($L/b = 8$) experienced a critical wave length at $\lambda/L = 2.2$; whereas the long hull evidently had not yet attained a critical wave length at $\lambda/L = 2.0$.

Potential Application of Results

The problem for both the seaplane pilot and the designer can be summarized:

1. To reduce as much as possible the amplitudes of the motion experienced by the seaplane. Eq 1 is rewritten here neglecting all coupling terms:

$$Q \frac{d^2s}{dt^2} + N \frac{ds}{dt} + R_s = F(s, t) .$$

The motion experienced by the seaplane subjected to the wave function, $F(s, t)$ is the result of the three reactions on the left-hand side of this equation. Any one of these reactions may be altered to influence the motion of the seaplane hull. The extent to which any one may be altered is determined by a complex compromise among all of the various functional requirements of the seaplane.

The inertial reaction, $Q \frac{d^2s}{dt^2}$, may be effected by the mass distribution and the distribution of the sectional areas of the hull. The damping reaction, $N \frac{ds}{dt}$, may be influenced by any one of a number of factors. Among these factors are:

1. The wave generation caused by the motion of the hull.
2. The energy dissipative eddies.
3. The passive damping caused by the aerodynamic surfaces of the wing and tail.
4. The active damping caused by pilot correction of particularly the pitching and rolling of the hull.

The restoring reaction, R_s, may be altered by distribution of the hull displacement both vertically and longitudinally.

In order to assess the findings of these experiments in a more specific manner, refer to the performance of the models as shown in Fig. 9. In the case of each motion (pitching, heaving or rolling), the motions move from relatively small values of amplitude factor to critical or peak values as the effective tuning ratio, Λ_e, is increased from either zero or small negative values to $\Lambda_e \cong 1.0$.

A rapid decrease in amplitude factor is experienced as the tuning ratio increases beyond the critical value. A second observation from Fig. 9 and also shown in Fig. 12 is that the amplitude factors are less when the relative wave lengths are smaller than two.

The amplitude factors accordingly are determined by the magnification factor, the tuning ratio and the relative wave length ratio. The design and/or operation of seaplanes from the seaworthiness point-of-view should be such that for the particular conditions existing the amplitude factors should be as small as possible.

To obtain the smallest possible amplitude factors, the magnification factor should be as small as practical. Stated in other words, the damping should be as high as possible. High damping may be achieved in different ways depending on the motion involved. Some undesirable ideas such as: (a) blunt bow and stern, (b) long, sharp chines, (c) sharp keel, and (d) horizontal fins at bow and stern are included among the methods of obtaining increased damping. One method is manipulation of elevator and ailerons to provide active damping of the pitching and rolling motions, particularly if these control surfaces happen to be in the slipstream.

Operation of the seaplane in the vicinity of synchronism ($\lambda_e \cong 1.0$) should be avoided. For a particular seaway this can be accomplished by

1. Change of heading - running with the waves if possible.
2. Changing the natural frequency of the hull -- particularly in the pitching motion.

An increase in the natural pitching frequency , ω_{n_τ} may be achieved by locating the concentrated masses as near the pitching axis as practical. If this could be accomplished, the critical tuning ratio ($\Lambda_e \cong 1.0$) would also occur at a higher value of frequency of encounter, ω_e . This is illustrated:

$$\Lambda_e = \frac{\omega_e}{\omega_n} = \frac{\omega - \frac{\omega_v \cos\chi}{c}}{\omega_n} ,$$

where

$$\omega_n \sim \frac{1}{K_L} ,$$

or

$$\omega_n = \frac{M}{K_L} ,$$

where K_L = longitudinal radius of gyration,

M = constant of proportionality,

hence,

$$\Lambda_e = \frac{\omega - \frac{\omega_v \cos\chi}{c}}{\frac{M}{K_L}}$$

From this relationship it can be seen that for a particular heading and wave length, the synchronism would occur at a higher speed. At a higher speed more of the weight of the seaplane is supported by aero-

dynamic lift. At a higher speed the pilot has more effective aerodynamic control and is in a better position to employ the active aerodynamic damping in pitch and roll previously referred to.

It has been observed that the model requires one or two wave encounters before reasonably steady oscillations are experienced. If the pilot could accelerate rapidly through the region of synchronism during the take-off run by using such special assistance as JATO, the extreme motion might be somewhat alleviated. During landing, rapid deceleration may be employed at the judicious moment by using reverse thrust.

These experiments and others reported in (1), (2) and (3) show that the amplitude factors tend to be highest when the wave-hull length ratio, λ/L , is between 1.0 and 2.2. Although no experiments could be conducted in waves longer than $\lambda/L = 2.4$, it can be reasoned that in extremely long waves the static water line will always be parallel to the wave slope and it is known that the steepness of the long waves is always low. Furthermore, their frequency, ω , is so low that most seaplane operations in these waves are far removed from synchronism. The problem exists with the wave from one to three times the hull length. These are waves from 80 to 250 ft in length having wave periods from approximately four to seven seconds or circular wave frequencies from 1.5 down to 0.9 radians per second. The relative wave length ratio, λ/L , may be reduced by increasing the length-beam ratio

for a particular seaplane size or by increasing the length and size of the seaplane. There are a number of other hydrodynamic and aerodynamic benefits to be gained from a higher length-beam ratio. In the event the wave conditions are such that the waves are from one to two times the hull length ($1.0 < \lambda/L < 2.0$) , the wave length may be effectively increased by travelling at some heading other than into or with the waves. The preferred heading is parallel to the wave crests ($\chi = 90^{\circ}$) since on this heading the relative wave length is infinity ($\frac{\lambda}{L \cos \chi} = \infty$) . It should be remembered, however, that if the wave length is approximately equal to the span between tip floats that the tip floats may be forced under when the hull is in the trough on this heading.

Performance of the Wing-Tip Floats

The wing-tip floats on the short hull appeared to be seriously submerged during some of the tests, particularly at the 45° , 90° and 135° headings. The float displacement of the shorter hull may have been inadequate for the requirements. Since the floats were scaled on the basis of the general hull dimensions, the displacement of the tip floats for the long hull ($L/b = 12$) was approximately 30 percent greater than for the short hull. In addition, the span between the floats was arbitrarily made equal to the hull length. This gave the tip floats for the short hull a potential static righting moment of 8.0 in-lb as compared to 13.5 in-lb for the long hull. Thus, the longer hull derived approximately 70 percent more support from its tip floats than the short hull.

VI. CONCLUSIONS

In summary the purposes of this project were:

1. To develop testing techniques.
2. To determine if the techniques used would differentiate between the behavior of the two models.

The experiments clearly showed the model having the high length-to-beam ratio to be more seaworthy. This is in accordance with the known facts so the conclusion may be drawn that the techniques were adequate to differentiate between the characteristics of the two models.

Specific results of the experiments will be discussed under three headings: (a) Testing techniques, (b) Motions of the models, and (c) Recommendations for design and operation.

Testing Techniques

The testing techniques were derived from existing procedures by considering obliquity to the wave front as an additional variable. The model was artificially unloaded as the testing speeds increased to simulate the increasing aerodynamic lift. It was towed by means of a bridle attached on a lateral axis through the center of gravity. Thus the model was restrained in yaw but unrestrained in all the other motions. (See Table 2 for a list of variables and their range of variation).

Recommendations for improvement:- Recommendations for improvement in testing procedure are as follows:

1. Increase the wave length used to 3.0 times the hull length. This can be accomplished by either increasing the size of the basin or reducing the size of the models.
2. Increase the speed range to at least $C_V = 8.0$, or to getaway speed.
3. Design instrumentation which will place the motion measurements on oscillograms so that all of the derivatives of the motion can be accurately determined.
4. Use color movie film to obtain clearer photographs of the spray envelopes.
5. Use dynamic self-powered models.

These recommendations toggther with the List of Variables (Table 2) may be considered to be a general set of specifications for seaworthiness testing in oblique seas.

Motions of the Models in Oblique Seas

The motions of the seaplane were described in terms of amplitude parameters. The pertinent factors affecting these are (a) the damping ratio, (b) the effective tuning ratio and (c) the relative wave-hull length ratio.

The seaworthiness, as measured by the pitching and heaving, was improved by increasing the length-to-beam ratio from 8 to 12 (see Fig. 9).

General Observations for Design and Operation

Based on observations of the tests and analysis of the data the following comments may be made as guides for the operation and design of seaplanes:

1. The critical values of the effective tuning ratio, λ_e, for the hulls tested are (see Fig. 9):

   Trim parameter - $0.75 < \omega_e/\omega_n < 0.85$,

   Heave parameter - $0.5 < \omega_e/\omega_n < 0.85$,

   Roll parameter - $0.6 < \omega_e/\omega_n < 1.7$.

2. Following are the headings on which maximum and minimum amplitude parameters of model motions were observed (see Fig. 10):

Motion	Minimum	Maximum
Pitching	90°, 0°	180°, 135°
Heaving	0°	135°, 180°
Rolling	0°	45°, 90°

3. Operation at speeds and on headings producing synchronism should be avoided if possible. In the case of the models tested, this could be accomplished by traveling with the waves (X = 0°) or parallel to the wave crests (X = 90°) (see Fig. 10).

4. Operation in waves having an effective wave-hull length ratio between one and two ($1.0 < \frac{\lambda}{L \cos x} < 2.0$) should be avoided if possible. The amplitude parameters of all

motions increase as the wave length increases to a value of approximately 2.2 times the hull length (see Fig. 12). As the relative wave length is further increased the amplitude parameters are reduced.

5. The tip floats take heavy drag loads for the 90° heading at relatively low speeds.

Recommendations for Improved Technique

The models and the wave lengths should be of such size that the relative wave length can be increased to approximately 3.0 times the hull length. This can be accomplished by either increasing the wave length generated or by reducing the size of the model tested.

Increasing the length of the wave generated would require that the over-all dimensions of the testing basin be increased so that the length of test run may be increased. On the 0° heading, at the higher speeds used in these tests, only two wave encounters could be obtained and these only by carefully controlling the time of release. The model seems to have attained stabilized oscillations in pitching and heaving when the period of encounter is 1.3 seconds. When the period of encounter is less than 1.0 second, probably two encounters are required before stabilized oscillations are obtained.

Some problems would arise from reduction of model size. The relative weight of a small model increases so that weight requirements soon limit size reductions. The trend is toward more elaborate instrumentation - all carried by the model. These instruments add more weight

and hence, require greater rather than smaller model size. Much effort is being expended toward new light-weight materials and toward simplified miniaturized instrumentation. Possibly the combination of these would permit reduction of model size and still allow installation of more elaborate instruments.

A complete dynamic model should be used. Only in this way can the aerodynamic effects of the wing and tail be added to the motion of the model. Testing a self-powered model would seem highly desirable, however, such requirements would add to the weight of the model.

The photographic technique for measuring the model motions requires considerable time for analysis. It is highly desirable to have movies of the experiments. On the other hand, it is more desirable to have the time history of wave profile, model motions, and model speed all on oscillographic records. Only by the latter method is it possible to properly obtain some of the derivatives of the motion such as the accelerations and the phase angles between the different motions. If the model motions are measured from movie film, the movies should be taken at speeds of from 30-100 frames per second. Color film lends itself to more accurate measurements of spray envelopes and wave profile along the hull than black and white film. This is now more feasible since color film having a relative speed of ASA 128 is now available.

These experiments indicate that the rolling motion of the seaplane is dominated by tip floats. It is believed that the location and size of the tip float should be further investigated.

REFERENCES

1. Benson, James M., Havens, Robert F., and Woodward, David R. Landing characteristics in waves of three dynamic models of flying boats. Washington, National Advisory Committee for Aeronautics. Tech. Note 2508, 1952.

2. Parkinson, J. B. Appreciation and determination of the hydrodynamic qualities of seaplanes. Washington, National Advisory Committee for Aeronautics. Tech. Note No. 1290, May 1947.

3. Parkinson, J. B. Model investigations of seaplanes in waves. Proc. First Conference on Ships and Waves, Richmond, California, October 1954.

4. Pierson, W. S., Jr., Neumann, G., and James, R. W. Practical methods for observing and forecasting ocean waves by means of wave spectra and statistics. New York, New York University. Tech. Rept. No. 1, Bureau of Aeronautics Project AROWA, July 1953.

5. Schulz, E. F. Development of a basin for investigation of the seaworthiness of model seaplane hulls. Fort Collins, Colorado A and M College, Civil Engineering Department Report No. 54EFS11, March 1954.

6. St. Denis, M. On sustained sea speed. Proc. Soc. Naval Architects and Marine Engineers, New York, November 1951.

7. St. Denis, M. and Pierson, W. J. On the motions of ships in confused seas. Proc. Soc. Naval Architects and Marine Engineers, New York, November 1953.

8. St. Denis, M. and Pierson, W. J. On some recent developments in the theory of ship motions. Proc. First Conference on Ships and Waves, Richmond, California, October 1954.

9. Wiegel, R. L. Gravity waves, Tables of functions. Council on Wave Research, Berkeley, California, February 1954.

10. Weinblum, G. and St. Denis, M. On the motions of ships at sea. Proc. Soc. Naval Architects and Marine Engineers, New York, November 1950.

FIGURES

TABLES

Table 1

MODEL PARTICULARS

	Model 1067-1	Model 1068-1
Beam, maximum, inches	6.12	5.02
Over-all length-to-beam ratio	8	12
Forebody length, inches	24.60	30.12
Afterbody length, inches	24.60	30.12
Total hull length, inches	49.20	60.24
Step depth (at keel), inches	0.37	0.30
Sternpost angle, degrees	8.0	8.0
Sternpost height, inches	3.09	3.92
Center of gravity position		
Forward from main step apex, inches	4.12	3.60
Above baseline, inches		
(1953 tests)	3.50	3.50
(1954 tests)	6.50	6.50
Span between tip floats, in.	48.0	60.0
Tip float volume, cubic inches	9.2	12.5
Gross load coefficient, C_{Δ}	2.5	4.7
Getaway speed coefficient	8.45	9.42

Table 2

LIST OF VARIABLES

Variable	Title	Range of Variation
L/b	Length-beam ratio	8 and 12
C_{Δ}	Load coefficient	for $L/b = 8$ - 1.5, 2.0, 2.5 for $L/b = 12$ - 2.8, 3.7, 4.7
λ	Wave length, ft.	4.2, 8.7, 9.7
λ/h	Height-length ratio	0.069, 0.030, 0.027
v	Model speed, fps	0, 3.2, 10.9, 11.6, 13.8
χ	Angle of heading	0, 45, 90, 135, 180°

Example of computation of mass moment of inertia

Period of a torsional pendulum

$$T = 2\pi\sqrt{\frac{I}{k}}$$

where T = period of oscillation in seconds

I = moment of inertia of mass suspended by wire

k = a constant which is related to the wire

The constant k is determined by observing the period of oscillation of a slender box suspended at its center of gravity and having approximately the same weight as the seaplane. The mass moment of inertia of the bar can be computed:

$$I_{bar} = M\frac{L^2}{12} = \frac{WL^2}{12g}$$

Observed period of seaplane (average of three trials) = 45.49 seconds. Wire constant, k = 0.00569.

$$I = \frac{0.00569}{4\pi^2}\ T^2 = 0.298 \text{ slug} - \text{ft}^2$$

Note: k is a constant as long as:

(1) the weight does not stress the wire beyond the elastic limit,

(2) the unit torsional deformation is small

(3) the air drag on the model is negligible

Table 3

MOMENT OF INERTIA OF MODELS

Axis	Δ (lb)	Model 1067-1 L/b = 8		Model 1068-1 L/b = 12	
		C_Δ	I Slug-ft^2	C_Δ	I Slug-ft^2
Vertical, z (yawing)	12.85	1.5	0.397	2.8	0.478
	17.05	2.0	0.384	3.8	0.484
	21.35	2.5	0.382	4.7	0.480
Lateral, y (pitching)	12.85	1.5	0.195	2.8	0.294
	17.05	2.0	0.217	3.8	0.310
	21.35	2.5	0.226	4.7	0.322
Longitudinal, x (rolling)	12.85	1.5	0.270	2.8	0.252
	17.05	2.0	0.298	3.8	0.290
	21.35	2.5	0.308	4.7	0.302

Note: The distribution of ballast in the models is achieved through a trial and error process. The consideration for the distribution of the ballast are listed below in order of their importance.

1. Position of center of gravity of loaded hull along longitudinal axis (x axis),
2. Position of center of gravity of loaded hull along vertical axis (z axis),
3. Position of center of gravity of loaded hull along lateral axis (y axis),
4. Pitching moment of inertia,
5. Rolling moment of inertia,
6. Yawing moment of inertia.

The first consideration is obtaining the proper location of the center of gravity. The mass moment of inertia is then checked by hanging the model as a torsional pendulum (sample computations are shown below). In the case of the yawing axis, no attempt was made to satisfy any specified value of yawing moment of inertia because the model seaplane was towed by means of a bridle and the yawing oscillations were not permitted to develop.

Table 4

EXPERIMENTAL RESULTS FOR L/b = 8

χ (deg)	ω	v (fps)	C_v	Theoretical c (fps)	$\frac{v \cos\chi}{c}$	$1-\alpha$	ω_e	λ (ft)	$\frac{\lambda}{L}$	h (ft)	$\frac{h}{\lambda}$	ϑ (deg)	Δz (ft)	$\frac{\Delta z}{h}$	$\frac{\omega_e}{\omega_{n(z)}}$	$\Delta\tau$ (deg)	$\frac{\Delta\tau}{\vartheta}$	$\frac{\omega_e}{\omega_{n\phi}}$	$\Delta\phi$ (deg)	$\frac{\Delta\phi}{\vartheta}$
C_Δ = 2.5																				
180	.843	0	0	6.07	0	1	0.843	7.16	1.79	0.341	.0476	16.6	0.19	0.56	0.383	9.8	0.59	--	--	--
"	.843	1.84	0.451	6.07	-0.303	1.303	1.098	7.16	1.79	0.366	.0511	17.7	0.27	0.74	0.503	9.5	0.54	--	--	--
"	.722	0	0	7.11	0	1	0.722	9.81	2.45	0.230	.0234	8.1	0	0	0.327	--	--	--	--	--
"	.722	1.84	0.451	7.11	-0.259	1.259	0.909	9.81	2.45	0.217	.0221	7.8	0.23	1.06	0.400	8.8	1.13	--	--	--
"	.995	0	0	5.15	0	1	0.995	5.16	1.29	0.295	.0572	20.0	0.10	0.34	0.452	8.2	0.41	--	--	--
"	.995	1.84	0.451	5.15	-0.358	1.358	1.351	5.16	1.29	0.298	.0572	20.0	0.16	0.54	0.616	9.0	0.45	--	--	--
0	1.106	0	0	4.70	0	1	1.106	4.18	1.05	0.285	.0682	23.8	0.10	0.35	0.503	7.5	0.32	--	1.5	0.06
"	1.106	1.84	0.451	4.70	+0.392	0.608	0.672	4.18	1.05	0.285	.0682	23.8	0.06	0.21	0.304	6.8	0.29	--	3.3	0.14
"	.769	0	0	6.68	0	1	0.769	8.64	2.16	0.265	.0307	10.7	0.23	0.75	0.349	7.9	0.74	--	1.3	0.12
"	.766	1.84	0.451	6.70	0.275	0.725	0.555	8.70	2.18	0.246	.0283	9.8	0.13	0.46	0.248	7.5	0.77	--	1.5	0.15
"	.726	0	0	7.07	0	1	0.726	9.69	2.42	0.215	.0222	7.8	0.19	0.88	0.330	7.8	1.00	--	1.5	0.19
"	.726	1.84	0.451	7.07	0.260	0.740	0.537	9.69	2.42	0.220	.0227	7.9	0.14	0.62	0.238	6.5	0.82	--	2.2	0.28
45	.726	0	0	7.07	0	1	0.726	9.69	2.42	0.207	.0214	7.5	0.23	1.11	0.330	5.5	0.73	0.790	11.0	1.47
"	.724	1.84	0.451	7.09	+0.183	0.817	0.592	9.75	2.44	0.225	.0231	8.0	0.23	1.02	0.244	5.7	0.68	0.584	13.2	1.65
"	.769	0	0	6.68	0	1	0.769	8.64	2.16	0.245	.0284	9.9	0.28	1.15	0.349	6.9	0.70	0.835	12.2	1.23
"	.763	1.84	0.451	6.73	0.193	0.807	0.616	8.78	2.20	0.263	.0300	10.4	0.17	0.65	0.276	5.4	0.52	0.661	7.2	0.69
"	1.106	0	0	4.70	0	1	1.106	4.18	1.05	0.296	.0708	24.7	0.14	0.47	0.503	8.0	0.32	1.200	1.0	0.04
"	1.106	1.84	0.451	4.70	0.276	0.724	0.801	4.18	1.05	0.301	.0720	25.0	0.15	0.50	0.362	7.2	0.29	0.867	5.2	0.21
135	1.106	0	0	4.70	0	1	1.106	4.18	1.05	0.293	.0710	24.8	--	--	0.503	8.5	0.34	1.200	1.5	0.06
"	1.106	1.84	0.451	4.70	-0.276	1.276	1.411	4.18	1.05	0.318	.0761	26.6	0.13	0.41	0.644	10.2	0.38	1.540	0	0
"	1.106	0	0	4.70	0	1	1.106	4.18	1.05	0.318	.0761	26.6	0.15	0.47	0.503	8.5	0.32	1.200	1.1	0.04
"	.769	0	0	6.68	0	1	0.769	8.64	2.16	0.261	.0302	10.4	0.23	0.88	0.349	8.0	0.77	0.836	9.8	0.94
"	.763	1.84	0.451	6.73	-0.193	1.193	0.910	8.78	2.20	0.275	.0313	10.9	0.27	0.98	0.416	7.8	0.72	0.996	--	--
"	.724	1.84	0.451	7.09	-0.183	1.183	0.856	9.75	2.44	0.218	.0224	7.8	0.23	1.05	0.389	5.9	0.76	0.930	2.9	0.37
"	.724	0	0	7.09	0	1	0.724	9.75	2.44	0.232	.0238	8.3	0.29	1.25	0.329	6.0	0.72	0.786	8.2	0.99
90	.726	0	0	7.07	0	1	0.726	9.69	2.42	0.269	.0278	9.8	0.30	1.11	0.330	0	0	0.790	3.2	0.33
"	.726	1.84	0.451	7.07	0	1	0.726	9.69	2.42	0.270	.0279	9.8	0.18	0.67	0.330	1.5	0.15	0.790	5.2	0.53
"	.766	0	0	6.70	0	1	0.766	8.70	2.18	0.264	.0304	10.5	0.18	0.68	0.348	1.6	0.15	0.834	6.4	0.61
"	.766	1.84	0.451	6.70	0	1	0.766	8.70	2.18	0.268	.0308	10.6	0.18	0.67	0.348	3.0	0.28	0.834	2.0	0.19
"	1.106	0	0	4.70	0	1	1.106	4.18	1.05	0.348	.0833	29.0	0.27	0.78	0.503	0.5	0.17	1.200	4.6	0.16
"	1.106	1.84	0.451	4.70	0	1	1.106	4.18	1.05	0.338	.0809	28.1	0.27	0.80	0.503	1.2	0.04	1.200	2.6	0.09
C_Δ = 2.0																				
90	1.106	0	0	4.70	0	1	1.106	4.18	1.05	0.331	.0791	27.6	0.25	0.76	0.500	0.9	0.03	1.479	4.6	0.17
"	1.106	3.16	0.777	4.70	0	1	1.106	4.18	1.05	0.336	.0804	28.0	0.21	0.63	0.500	0.6	0.02	1.479	6.9	0.25
"	1.106	11.15	2.74	4.70	0	1	1.106	4.18	1.05	0.333	.0796	27.8	0.24	0.72	0.500	0	0	1.479	4.5	0.16
"	.763	0	0	6.73	0	1	0.763	8.78	2.20	0.250	.0285	10.0	0.17	0.68	0.346	1.5	0.15	1.021	13.3	1.33
"	.763	3.18	0.782	6.73	0	1	0.763	8.78	2.20	0.253	.0288	10.0	0.23	0.91	0.346	1.3	0.13	1.021	--	--
"	.763	11.74	2.89	6.73	0	1	0.763	8.78	2.20	0.253	.0288	10.0	0.26	1.03	0.346	2.6	0.25	1.021	9.5	0.92
"	.722	0	0	7.11	0	1	0.722	9.81	2.45	0.243	.0248	8.7	0.24	0.99	0.327	2.0	0.23	0.965	12.5	1.44
"	.726	3.17	0.779	7.07	0	1	0.726	9.69	2.42	0.233	.0241	8.3	0.21	0.90	0.329	1.0	0.12	0.972	10.4	1.25
"	.724	11.70	2.88	7.09	0	1	0.724	9.75	2.44	0.269	.0276	9.6	0.23	0.86	0.327	3.8	0.40	0.968	10.0	1.04

Table 4 --Continued

L/b = 8

χ (deg)	ω	v (fps)	C_v	Theoretical c (fps)	$\frac{v \cos\chi}{c}$	$1-\alpha$	ω_e	λ (ft)	$\frac{\lambda}{L}$	$\frac{h}{\lambda}$	h (ft)	ϑ (deg)	Δz (ft)	$\frac{\Delta z}{h}$	$\frac{\omega_e}{\omega_{n(z)}}$	$\Delta\tau$ (deg)	$\frac{\Delta\tau}{\vartheta}$	$\frac{\omega_e}{\omega_{n\phi}}$	$\Delta\phi$ (deg)	$\frac{\Delta\phi}{\vartheta}$
C_Δ = 2.0																				
135	.726	0	0	7.07	0	1	0.726	9.69	2.42	0.191	.0197	6.8	0.19	1.02	0.329	6.7	0.99	0.972	12.6	1.85
"	.726	3.17	0.779	7.07	-0.448	1.448	1.051	9.69	2.42	0.200	.0206	7.1	0.23	1.14	0.439	6.2	0.86	1.299	5.0	0.69
"	.726	10.5	2.58	7.07	-1.485	2.485	1.804	9.69	2.42	0.200	.0206	7.1	0.17	0.84	0.695	6.6	0.92	2.055	6.7	0.94
"	.766	0	0	6.70	0	1	0.766	8.70	2.18	0.255	.0293	10.1	0.22	0.87	0.347	7.6	0.75	1.025	11.7	1.16
"	.766	3.19	0.784	6.70	-0.336	1.336	1.023	8.70	2.18	0.255	.0293	10.1	0.21	0.82	0.470	8.9	0.88	1.388	4.6	0.45
"	.766	11.2	2.76	6.70	-1.182	2.182	1.671	8.70	2.18	0.259	.0298	10.3	--	--	0.284	29.3	2.36	2.285	4.4	0.43
"	1.106	0	0	4.70	0	1	1.106	4.18	1.05	0.280	.0670	23.3	0.07	0.25	0.50	9.2	0.40	1.479	0.6	0.03
"	1.106	3.19	0.784	4.70	-0.480	1.480	1.637	4.18	1.05	0.305	.0730	25.4	0.17	0.56	0.742	11.0	0.43	2.19	1.8	0.07
"	1.106	11.65	2.86	4.70	-1.753	2.753	3.045	4.18	1.05	0.310	.0742	25.8	0.07	0.23	1.383	8.9	0.35	4.09	2.2	0.09
45	1.106	0	0	4.70	0	1	1.106	4.18	1.05	0.305	.0730	25.4	0.13	0.43	0.50	9.5	0.37	1.479	0.5	0.02
"	1.106	3.21	0.789	4.70	+0.483	0.517	0.572	4.18	1.05	0.315	.0754	26.3	0.01	0.03	0.260	7.5	0.28	0.770	6.3	0.24
"	1.106	10.8	2.66	4.70	+1.625	-0.675	-0.747	4.18	1.05	0.301	.0720	25.1	0.16	0.54	0.323	2.8	0.11	-0.953	--	--
"	.766	0	0	6.70	0	1	0.766	8.70	2.18	0.263	.0302	10.4	0.18	0.69	0.347	6.5	0.62	1.025	4.7	0.45
"	.769	3.13	0.771	6.68	0.331	0.669	0.514	8.64	2.16	0.269	.0254	8.8	0.36	1.34	0.226	5.7	0.65	0.669	--	--
"	.772	9.63	2.37	6.65	1.024	-0.024	-0.019	8.58	2.15	0.276	.0322	11.2	--	--	-0.028	0.1	0.09	-0.0843	1.4	0.13
"	.769	3.15	0.775	6.68	0.333	0.667	0.513	8.64	2.16	0.277	.0321	11.1	--	--	0.226	--	--	0.667	--	--
"	.726	0	0	7.07	0	1	0.726	9.69	2.42	0.205	.0212	7.4	0.25	1.22	0.329	5.1	0.69	0.972	10.9	1.48
"	.726	3.16	0.777	7.07	0.316	0.684	0.497	9.69	2.42	0.220	.0227	7.9	0.25	1.14	0.218	4.9	0.62	0.645	16.5	2.09
"	.724	11.4	2.80	7.09	1.136	-0.136	-0.098	9.75	2.44	0.230	.0236	8.2	0	0	-0.068	0.5	0.06	-0.202	2.4	0.29
180	.726	0	0	7.07	0	1	0.726	9.69	2.42	0.264	.0272	9.5	0.18	0.68	0.329	7.4	0.78	--	2.4	0.25
"	.726	3.21	0.789	7.07	-0.455	1.455	1.056	9.69	2.42	0.255	.0263	9.1	0.24	0.94	0.488	8.5	0.93	--	3.6	0.40
"	.726	12.9	3.17	7.07	-1.830	2.830	2.055	9.69	2.42	0.263	.0272	9.5	0.22	0.84	0.966	17.3	1.82	--	3.1	0.33
"	.772	0	0	6.65	0	1	0.772	8.58	2.15	0.289	.0337	11.7	0.25	0.87	0.349	9.2	0.79	--	4.2	0.36
"	.763	3.19	0.784	6.73	-0.475	1.475	1.125	8.78	2.20	0.259	.0295	10.2	0.30	1.16	0.518	8.5	0.83	--	2.5	0.25
"	.766	12.55	3.07	6.70	-1.87	2.87	2.198	8.70	2.18	0.298	.0343	11.9	0.39	1.31	1.028	16.6	1.40	--	4.7	0.40
"	1.106	0	0	4.70	0	1	1.106	4.18	1.05	0.332	.0795	27.6	0.07	0.21	0.500	8.6	0.31	--	6.6	0.24
"	1.106	3.19	0.784	4.70	-0.679	1.679	1.857	4.18	1.05	0.335	.0800	27.9	0.14	0.42	0.843	14.0	0.50	--	1.2	0.04
"	1.106	11.65	2.86	4.70	-2.480	3.480	3.849	4.18	1.05	0.370	.0885	30.9	0.09	0.24	1.755	4.0	0.13	--	0	0
0	1.112	0	0	4.67	0	1	1.112	4.12	1.03	--	--	21.6	0.02	0.08	0.504	7.5	0.35	--	6.5	0.30
"	1.112	3.21	0.789	4.67	+0.687	0.313	0.348	4.12	1.03	0.255	.0620	21.6	0.08	0.31	1.591	2.5	0.12	--	4.7	0.22
"	1.106	10.6	2.60	4.70	2.255	-1.255	-1.388	4.18	1.05	0.329	.0787	27.3	0.16	0.50	-0.640	7.4	0.27	--	1.2	0.04
"	.763	0	0	6.73	0	1	0.763	8.78	2.20	0.277	.0316	11.0	0.22	0.80	0.345	8.6	0.78	--	4.4	0.40
"	.766	3.17	0.779	6.70	0.473	0.527	0.404	8.70	2.18	0.238	.0374	13.0	0.09	0.38	0.175	8.4	0.65	--	3.1	0.24
"	.763	11.6	2.85	6.73	1.723	-0.723	-0.552	8.78	2.20	0.233	.0265	9.2	0.16	0.69	-0.278	9.0	0.98	--	2.1	0.23
"	.724	0	0	7.09	0	1	0.724	9.75	2.44	0.263	.0270	9.3	0.20	0.76	0.328	7.5	0.81	--	5.0	0.54
"	.724	3.21	0.789	7.09	0.453	0.547	0.396	9.75	2.44	0.213	.0218	7.6	0	0	0.170	7.0	0.92	--	3.2	0.42
"	.726	11.15	2.74	7.07	1.578	-0.578	-0.420	9.69	2.42	0.253	.0262	9.1	0.04	0.16	-0.223	5.0	0.55	--	3.2	0.35
C_Δ = 1.5																				
180	.726	10.9	2.68	7.07	-1.54	2.54	1.844	9.69	2.42	0.215	.0222	7.8	0.22	0.98	0.855	17.4	2.23	--	5.9	0.76
"	.726	13.9	3.42	7.07	-1.97	2.97	2.156	9.69	2.42	0.213	.0220	7.7	--	--	1.000	16.0	2.08	--	14.7	1.91
"	.769	10.9	2.68	6.68	-1.63	2.63	2.022	8.64	2.16	0.240	.0278	9.6	0.51	2.12	0.934	23.2	2.42	--	8.3	0.87
"	.766	13.7	3.37	6.70	-2.05	3.05	2.336	8.70	2.18	0.238	.0274	9.5	0.38	1.59	1.074	16.0	1.68	--	11.8	1.24
"	1.112	11.84	2.91	4.67	-2.54	3.54	3.936	4.12	1.03	0.288	.0699	24.4	0.08	0.28	1.770	4.8	0.20	--	1.5	0.06
"	1.097	13.95	3.43	4.72	-2.96	3.96	4.344	4.23	1.06	0.285	.0674	23.3	0.10	0.35	1.949	3.2	0.14	--	2.2	0.09

Table 4 --Continued

L/b = 8

χ (deg)	ω	v (fps)	C_v	Theoretical c (fps)	$\frac{v\cos\chi}{c}$	$1-\alpha$	ωe	λ (ft)	$\frac{\lambda}{L}$	h (ft)	$\frac{h}{\lambda}$	τ^2 (deg)	Δz (ft)	$\frac{\Delta z}{h}$	$\frac{\omega e}{\omega n(z)}$	$\Delta\tau$ (deg)	$\frac{\Delta\tau}{\tau^2}$	$\frac{\omega e}{\omega n\phi}$	$\Delta\phi$ (deg)	$\frac{\Delta\phi}{\tau^2}$
C_A = 1.5																				
0	1.106	9.9	2.43	4.70	+2.10	-1.10	-1.217	4.18	1.05	0.295	.0705	24.6	0.28	0.96	-0.539	5.0	0.20	--	1.4	0.06
"	1.106	12.4	3.04	4.70	2.64	-1.64	-1.814	4.18	1.05	0.299	.0715	24.9	--	0.58	-0.824	--	--	--	5.6	0.23
"	.766	10.7	2.63	6.70	1.60	-0.60	-0.460	8.70	2.18	0.288	.0331	11.3	0.15	0.52	-0.229	6.5	0.58	--	1.7	0.15
"	.769	13.3	3.27	6.68	1.99	-0.99	-0.761	8.64	2.16	0.276	.0320	11.1	0.14	0.51	-0.374	4.0	0.36	--	7.5	0.68
"	.722	10.8	2.66	7.11	1.52	-0.52	-0.375	9.81	2.45	0.234	.0238	8.3	0.05	0.21	-0.196	5.7	0.69	--	4.0	0.48
"	.722	13.5	3.32	7.11	1.90	-0.90	-0.650	9.81	2.45	0.223	.0227	7.9	0.12	0.53	-0.328	3.2	0.40	--	2.9	0.37
90	1.106	10.7	2.63	4.70	0	1	1.106	4.18	1.05	0.339	.0810	28.3	0.15	0.44	0.493	0.5	0.02	1.725	4.3	0.15
"	1.112	13.6	3.35	4.67	0	1	1.112	4.12	1.03	0.331	.0805	28.0	0.26	0.79	0.497	2.7	0.10	1.740	16.2	0.58
"	0.769	10.7	2.63	6.68	0	1	0.769	8.64	2.16	0.256	.0297	10.3	0.10	0.34	0.343	2.3	0.22	1.200	10.5	1.02
"	.763	13.4	3.30	6.73	0	1	0.763	8.78	2.20	0.255	.0290	10.0	--	--	0.340	7.0	0.70	1.190	15.5	1.55
"	.722	10.8	2.66	7.11	0	1	0.722	9.81	2.45	0.254	.0259	9.0	0.22	0.87	0.322	4.0	0.45	1.129	9.7	1.08
"	.726	13.4	3.30	7.07	0	1	0.726	9.69	2.42	0.261	.0270	9.3	0.15	0.58	0.324	5.6	0.60	1.133	11.0	0.86
135	.722	10.8	2.66	7.11	-1.072	2.072	1.496	9.81	2.45	0.273	.0278	9.6	0.30	1.10	0.690	10.5	1.09	2.419	8.3	0.87
"	.722	13.4	3.30	7.11	-1.330	2.330	1.682	9.81	2.45	0.273	.0278	9.6	0.44	1.60	0.776	14.0	1.46	2.720	6.0	0.63
"	.772	10.7	2.63	6.65	-1.137	2.137	1.650	8.58	2.15	0.270	.0315	10.9	0.28	1.04	0.759	15.7	1.44	2.655	5.6	0.51
"	.769	13.3	3.27	6.68	-1.410	2.410	1.853	8.64	2.16	0.245	.0284	9.8	0.43	1.77	0.850	19.5	1.99	2.980	2.1	0.22
"	1.106	10.7	2.63	4.70	-1.610	2.610	2.887	4.18	1.05	0.330	.0790	27.5	0.10	0.30	1.299	10.5	0.38	4.549	3.2	0.12
"	1.106	13.1	3.22	4.70	-1.970	2.970	3.285	4.18	1.05	0.361	.0863	30.1	0.10	0.28	1.431	5.6	0.19	5.020	3.4	0.11
45	1.097	10.5	2.58	4.72	+1.57	-0.57	-0.625	4.23	1.06	0.337	.0797	27.8	0.10	0.30	-0.288	5.4	0.19	-1.010	6.4	0.23
"	1.106	11.9	2.92	4.70	1.790	-0.790	-0.874	4.18	1.05	0.330	.0788	27.5	--	--	-0.401	--	--	-1.405	--	--
"	1.097	10.8	2.66	4.72	1.618	-0.618	-0.678	4.23	1.06	0.286	.0675	23.6	0.09	0.32	-0.308	--	--	-1.078	8.9	0.37
"	1.112	11.2	2.76	4.67	1.694	-0.694	-0.772	4.12	1.03	0.281	.0681	23.7	0	0	-0.352	--	--	-1.235	10.6	0.45
"	0.763	10.2	2.50	6.73	1.070	-0.070	-0.053	8.78	2.20	0.262	.0298	10.3	0	0	-0.409	0.6	0.06	-1.430	--	--
"	0.769	11.2	2.76	6.68	1.1188	-0.1188	-0.092	8.64	2.16	0.272	.0315	11.0	--	--	-0.086	8.6	0.78	-0.300	1.3	0.12
"	0.726	10.3	2.53	7.07	1.030	-0.030	-0.022	9.69	2.42	0.215	.0222	7.8	0	0	-0.031	1.3	0.17	-0.108	4.5	0.58
"	0.726	11.45	2.81	7.07	1.145	-0.145	-0.105	9.69	2.42	0.204	.0210	7.4	0	0	-0.071	4.4	0.60	-0.250	2.7	0.37

Table 4 --Continued

EXPERIMENTAL RESULTS FOR L/b = 12

χ (deg)	ω	v (fps)	C_v	Theoretical c (fps)	$\frac{v \cos \chi}{c}$	$1-\alpha$	ω_e	λ (ft)	$\frac{\lambda}{L}$	h (ft)	$\frac{h}{\lambda}$	ν° (deg)	Δz (ft)	$\frac{\Delta z}{h}$	$\frac{\omega_e}{\omega_{n(z)}}$	$\Delta\tau$ (deg)	$\frac{\Delta\tau}{\nu^\circ}$	$\frac{\omega_e}{\omega_{n\phi}}$	$\Delta\phi$ (deg)	$\frac{\Delta\phi}{\nu^\circ}$
C_Δ = 2.8																				
0	0.726	10.85	2.95	7.07	1.536	-0.536	-0.389	9.69	1.94	0.209	.0216	7.5	0.10	0.48	-0.165	9.0	1.20	-0.480	4.1	0.55
"	.724	13.45	3.66	7.09	1.900	-0.900	-0.650	9.75	1.95	0.213	.0218	7.6	0.24	1.12	-0.275	--	--	-0.802	5.6	0.74
"	.769	10.80	2.94	6.68	1.618	-0.618	-0.475	8.64	1.73	0.218	.0252	8.7	0.18	0.84	-0.201	5.6	0.64	-0.586	3.0	0.35
"	.769	13.50	3.68	6.68	2.025	-1.025	-0.787	8.64	1.73	0.235	.0272	9.4	0.19	0.79	-0.333	2.0	0.21	-0.972	2.4	0.26
"	1.106	10.85	2.95	4.70	2.305	-1.305	-1.442	4.18	0.84	0.292	.0698	24.3	0.10	0.34	-0.611	5.3	0.22	-1.780	8.6	0.35
"	1.106	13.65	3.71	4.70	2.905	-1.905	-2.110	4.18	0.84	0.318	.0762	26.7	0.03	0.16	-0.894	--	--	-2.605	3.5	0.13
180	1.097	10.7	2.91	4.72	-2.270	3.270	3.585	4.23	0.85	0.300	.0709	24.7	0	0	1.519	2.0	0.08	4.426	0.7	0.03
"	1.106	13.35	3.64	4.70	-2.840	3.840	4.250	4.18	0.84	0.302	.0723	25.2	0.08	0.27	1.801	1.5	0.06	5.247	1.0	0.04
"	0.772	10.6	2.88	6.65	-1.594	2.594	2.000	8.58	1.72	0.238	.0278	9.7	0.22	0.93	0.874	20.0	2.06	2.469	--	--
"	.769	12.9	3.52	6.68	-1.932	2.932	2.255	8.64	1.73	0.240	.0278	9.7	0.16	0.67	0.956	16.5	1.70	2.784	--	--
"	.724	10.65	2.90	7.09	-1.503	2.503	1.810	9.75	1.95	0.214	.0220	7.7	0.17	0.80	0.767	14.0	1.82	2.235	4.5	0.59
"	.722	12.9	3.52	7.11	-1.816	2.816	2.030	9.81	1.96	0.218	.0222	7.8	0.18	0.83	0.860	12.5	1.60	2.506	11.6	1.49
90	0.726	10.95	2.99	7.07	0	1	0.726	9.69	1.94	0.246	.0254	8.9	0.41	1.64	0.308	2.4	0.27	0.896	10.0	1.12
"	.724	14.0	3.81	7.09	0	1	0.724	9.75	1.95	0.250	.0256	8.9	0.07	0.28	0.307	1.4	0.16	0.894	12.3	1.38
"	.766	10.95	2.99	6.70	0	1	0.766	8.70	1.74	0.290	.0333	11.5	0.11	0.38	0.325	4.0	0.35	0.946	11.2	0.98
"	.763	13.9	3.78	6.73	0	1	0.763	8.78	1.76	0.260	.0296	10.3	0.22	0.85	0.323	3.5	0.34	0.942	12.5	1.21
"	1.106	10.85	2.95	4.70	0	1	1.106	4.18	0.84	0.343	.0822	28.6	0.24	0.70	0.469	2.0	0.07	1.365	12.0	0.42
"	1.106	13.4	3.65	4.70	0	1	1.106	4.18	0.84	0.361	.0865	30.1	0.15	0.42	0.469	3.0	0.10	1.365	7.0	0.23
135	0.726	10.55	2.86	7.07	-1.494	2.494	1.809	9.69	1.94	0.230	.0247	8.6	0.42	1.77	0.767	8.5	0.99	2.233	7.5	0.82
"	.726	13.9	3.78	7.07	-1.967	2.967	2.155	9.69	1.94	0.239	.0247	8.6	0.35	1.46	0.913	11.2	1.30	2.660	8.6	1.00
"	.769	10.55	2.86	6.68	-1.117	2.117	1.625	8.64	1.73	0.278	.0322	11.3	0.28	1.00	0.689	12.3	1.09	2.006	4.9	0.43
"	.769	13.7	3.73	6.68	-1.450	2.450	1.883	8.64	1.73	0.281	.0325	11.3	--	--	0.798	--	--	2.325	--	--
"	.772	13.9	3.78	6.65	-1.478	2.478	1.910	8.58	1.72	0.260	.0303	10.4	--	--	0.809	--	--	2.358	0.7	0.07
"	1.097	10.6	2.88	4.72	-1.589	2.589	2.840	4.23	0.85	0.292	.0690	24.0	--	--	1.203	--	--	3.506	--	--
"	1.106	10.5	2.58	4.70	-1.580	2.580	2.855	4.18	0.84	0.292	.0698	24.4	0.02	0.07	1.210	7.0	0.29	3.525	1.2	0.05
"	1.112	13.8	3.76	4.67	-2.090	3.090	3.440	4.12	0.82	0.284	.0690	24.0	0.09	0.32	1.458	4.6	0.19	4.247	2.7	0.11
45	1.106	10.3	2.79	4.70	1.548	-0.548	-0.607	4.18	0.84	0.303	.0725	25.2	0.12	0.40	-0.257	5.5	0.22	-0.749	9.8	0.39
"	1.106	11.75	3.19	4.70	1.768	-0.768	-0.850	4.18	0.84	0.307	.0735	25.6	--	0.63	-0.360	5.2	0.20	-1.049	7.4	0.29
"	.766	10.4	2.82	6.70	1.098	-0.098	-0.075	8.70	1.74	0.248	.0285	10.0	0	0	-0.032	1.4	0.14	-0.093	5.1	0.51
"	.769	13.5	3.68	6.68	1.430	-0.430	-0.331	8.64	1.73	0.263	.0304	10.5	0.10	0.39	-0.140	--	--	-0.409	--	--
"	.726	10.5	2.85	7.07	1.487	-0.487	-0.353	9.69	1.94	0.203	.0210	7.3	0	0	-0.150	2.5	0.34	-0.436	5.5	0.75
"	.726	13.7	3.73	7.07	1.938	-0.938	-0.680	9.69	1.94	0.226	.0234	8.2	0.08	0.35	-0.288	2.6	0.32	-0.840	10.5	1.28
"	1.106	13.4	3.65	4.70	2.015	-1.015	-1.123	4.18	0.84	0.283	.0677	23.6	0.06	0.21	-0.476	5.3	0.22	-1.386	8.4	0.36
C_Δ = 3.75																				
90	0.722	0	0	7.11	0	1	0.722	9.81	1.96	0.214	.0218	7.6	0.32	1.51	0.313	0.9	0.12	0.818	8.7	1.15
"	.722	3.20	0.877	7.11	0	1	0.722	9.81	1.96	0.225	.0229	8.0	0.27	1.20	0.313	1.3	0.16	0.818	13.0	1.63
"	.726	12.9	3.52	7.07	0	1	0.726	9.69	1.94	0.230	.0238	8.2	0.57	0.25	0.314	1.9	0.23	0.822	5.7	0.70
"	.772	0	0	6.65	0	1	0.772	8.58	1.72	0.252	.0294	10.3	0.14	0.56	0.334	1.5	0.15	0.874	10.9	1.06
"	.769	3.17	0.870	6.68	0	1	0.769	8.64	1.73	0.245	.0284	9.9	0.26	1.06	0.333	0.3	0.03	0.871	10.9	1.10
"	.769	12.9	3.52	6.68	0	1	0.769	8.64	1.73	0.226	.0262	9.1	0.19	0.84	0.333	2.0	0.22	0.871	9.4	1.03
"	1.106	0	0	4.70	0	1	1.106	4.18	0.84	0.320	.0766	26.8	0.23	0.72	0.479	0.3	0.01	1.253	11.1	0.42
"	1.106	3.17	0.870	4.70	0	1	1.106	4.18	0.84	0.316	.0757	26.3	0.22	0.70	0.479	0.3	0.01	1.253	4.7	0.18
"	1.106	12.9	3.52	4.70	0	1	1.106	4.18	0.84	0.316	.0757	26.3	0.15	0.48	0.479	1.5	0.06	1.253	10.0	0.38

Table 4 --Continued

L/b = 12

χ (deg)	ω	v (fps)	C_v	Theoretical c (fps)	$v \cos\chi / c$	$1 - \alpha$	ω_e	λ (ft)	$\frac{\lambda}{L}$	h (ft)	$\frac{h}{\lambda}$	ϑ (deg)	Δz (ft)	$\frac{\Delta z}{h}$	$\frac{\omega_e}{\omega_{n(z)}}$	$\Delta\tau$ (deg)	$\frac{\Delta\tau}{\vartheta}$	$\frac{\omega_e}{\omega_{n\phi}}$	$\Delta\phi$ (deg)	$\frac{\Delta\phi}{\vartheta}$
C_Δ = 3.75																				
45	0.726	0	0	7.07	0	1	0.726	9.69	1.94	0.203	.0210	7.3	0.20	0.98	0.314	7.0	0.96	0.822	9.9	1.35
"	.724	3.18	0.872	7.09	+0.317	0.683	0.494	9.75	1.95	0.198	.0204	7.1	0.10	0.51	0.214	3.6	0.51	0.559	13.2	1.86
"	.724	12.8	3.49	7.09	+1.278	-0.278	-0.201	9.75	1.95	0.214	.0220	7.7	0.06	0.28	-0.087	2.2	0.29	-0.228	4.8	0.62
"	.769	0	0	6.68	0	1	0.769	8.64	1.73	0.251	.0291	10.1	0.19	0.76	0.333	7.1	0.71	0.871	10.4	1.03
"	.772	3.17	0.870	6.65	+0.336	0.667	0.515	8.58	1.72	0.242	.0282	9.9	0.10	0.42	0.223	6.2	0.63	0.583	10.7	1.08
"	.766	11.4	3.10	6.70	+1.203	-0.203	-0.155	8.70	1.74	0.284	.0327	11.4	0.09	0.32	-0.067	0.8	0.07	-0.176	0.9	0.08
"	1.106	0	0	4.70	0	1	1.106	4.18	0.84	0.312	.0746	26.0	0.09	0.29	0.479	7.6	0.29	1.253	11.5	0.44
"	1.106	3.18	0.872	4.70	+0.478	0.522	0.578	4.18	0.84	0.306	.0732	25.4	0.03	0.10	0.250	7.0	0.28	0.655	13.0	0.51
"	1.106	12.15	3.31	4.70	+1.828	-0.828	-0.916	4.18	0.84	0.307	.0735	25.6	0.06	0.20	-0.397	5.2	0.20	-1.037	10.0	0.39
135	1.106	0	0	4.70	0	1	1.106	4.18	0.84	0.300	.0719	25.0	0.08	0.27	0.479	8.5	0.34	1.253	13.2	0.53
"	1.106	3.18	0.872	4.70	-0.478	1.478	1.635	4.18	0.84	0.297	.0711	24.8	0.19	0.64	0.708	8.8	0.29	1.852	7.5	0.30
"	1.106	11.25	3.06	4.70	-1.691	2.691	2.98	4.18	0.84	0.290	.0695	24.2	0	0	1.290	6.3	0.26	3.375	1.2	0.05
"	0.766	0	0	6.70	0	1	0.766	8.70	1.74	0.244	.0281	9.8	0.21	0.86	0.332	8.0	0.34	0.867	9.0	0.92
"	.766	3.20	0.877	6.70	-0.338	1.338	1.023	8.70	1.74	0.256	.0294	10.2	0.29	1.12	0.443	7.4	0.73	1.159	5.4	0.53
"	.763	11.6	3.15	6.73	-1.219	2.219	1.690	8.78	1.76	0.304	.0347	12.0	0.39	1.29	0.732	16.4	1.37	1.914	2.0	0.17
"	.722	0	0	7.11	0	1	0.722	9.81	1.96	0.212	.0216	7.6	0.20	0.95	0.313	5.0	0.66	0.818	10.1	1.33
"	.724	3.16	0.867	7.09	-0.315	1.315	0.950	9.75	1.95	0.210	.0215	7.5	0.27	1.30	0.411	6.0	0.80	1.076	5.4	0.72
"	.726	11.9	3.24	7.07	-1.190	2.190	1.589	9.69	1.94	0.225	.0233	8.1	0.37	1.64	0.688	11.8	1.46	1.800	6.5	0.80
0	0.726	0	0	7.07	0	1	0.726	9.69	1.94	0.203	.0210	7.3	0.15	0.74	0.314	6.6	0.91	0.822	8.0	1.04
"	.726	3.21	0.880	7.07	+0.455	0.545	0.396	9.69	1.94	0.207	.0214	7.5	0.09	0.43	0.171	3.0	0.40	0.448	5.1	0.68
"	.726	12.5	3.40	7.07	+1.769	-0.769	-0.558	9.69	1.94	0.217	.0224	7.9	0.14	0.64	-0.242	--	--	-0.632	2.9	0.37
"	.769	0	0	6.68	0	1	0.769	8.64	1.73	0.246	.0285	10.0	0.22	0.90	0.333	8.2	0.82	0.871	5.6	0.56
"	.763	3.21	0.880	6.73	+0.477	0.523	0.399	8.78	1.76	0.247	.0281	9.8	0.15	0.61	0.173	5.4	0.55	0.452	3.7	0.38
"	.766	12.15	3.31	6.70	+1.813	-0.813	-0.623	8.70	1.74	0.250	.0288	10.0	0.16	0.64	-0.270	4.6	0.46	-0.706	0.9	0.09
"	1.106	0	0	4.70	0	1	1.106	4.18	0.84	0.297	.0710	24.7	0.02	0.07	0.479	5.5	0.22	1.253	7.9	0.32
"	1.106	3.21	0.880	4.70	+0.683	0.317	0.350	4.18	0.84	0.291	.0697	24.3	0	0	0.152	3.0	0.12	0.396	4.7	0.19
"	1.097	11.5	3.13	4.72	+2.435	-1.435	-1.573	4.23	0.85	0.306	.0723	25.3	0.02	0.07	-0.681	4.5	0.18	-1.781	4.4	0.17
180	1.106	0	0	4.70	0	1	1.106	4.18	0.84	0.300	.0718	25.0	0.05	0.17	0.479	5.9	0.24	1.253	6.6	0.26
"	1.106	3.21	0.880	4.70	-0.683	1.683	1.861	4.18	0.84	0.295	.0706	24.6	0.06	0.20	0.806	8.4	0.34	2.108	8.2	0.33
"	1.106	11.2	3.05	4.70	-2.385	3.385	3.745	4.18	0.84	0.314	.0751	26.2	0	0	1.621	2.7	0.10	4.241	0.5	0.02
"	0.772	0	0	6.65	0	1	0.772	8.58	1.72	0.243	.0283	9.9	0.15	0.62	0.334	8.2	0.83	0.874	4.0	0.40
"	.766	3.22	0.882	6.70	-0.481	1.481	1.138	8.70	1.74	0.248	.0285	10.0	0.20	0.81	0.493	10.0	1.00	1.289	4.0	0.40
"	.766	10.4	2.82	6.70	-1.553	2.553	1.955	8.70	1.74	0.224	.0258	9.0	0.15	0.67	0.846	19.9	0.22	2.214	2.4	0.27
"	.724	0	0	7.09	0	1	0.724	9.75	1.95	0.218	.0224	7.9	0.14	0.64	0.313	6.7	0.85	0.820	3.0	0.38
"	.724	3.18	0.872	7.09	-0.449	1.449	1.049	9.75	1.95	0.220	.0226	7.9	0.15	0.68	0.454	7.0	0.89	1.188	2.1	0.27
"	.726	9.98	2.73	7.07	-1.410	2.410	1.742	9.69	1.94	0.220	.0226	7.9	0.17	0.77	0.754	15.2	1.92	1.973	2.5	0.32
C_Δ = 4.7																				
180	1.006	0	0	5.09	0	1	1.006	5.05	1.01	0.275	.0545	19.0	0.04	0.15	0.437	5.9	0.31	0.898	--	-
"	1.008	1.84	0.507	5.07	-0.362	1.362	1.371	5.03	1.01	0.307	.0610	21.3	0.10	0.33	0.596	7.0	0.33	1.224	--	-
"	.843	0	0	6.07	0	1	0.843	7.16	1.43	0.356	.0498	17.3	0.17	0.48	0.367	7.5	0.43	0.753	--	--
"	.843	1.84	0.507	6.07	-0.303	1.303	1.099	7.16	1.43	0.336	.0469	16.3	0.20	0.60	0.478	10.2	0.63	0.981	--	--
"	.722	0	0	7.11	0	1	0.722	9.81	1.96	0.230	.0235	8.2	0.21	0.91	0.314	7.5	0.92	0.645	--	--
"	.726	1.84	0.507	7.07	-0.260	1.260	0.915	9.69	1.94	0.237	.0245	8.6	0.20	0.85	0.398	7.2	0.84	0.817	--	--

Table 4 --Continued

L/b = 12

χ (deg)	ω	v (fps)	C_v	Theoretical c (fps)	$\frac{v \cos\chi}{c}$	$1-\alpha$	ω_e	λ (ft)	$\frac{\lambda}{L}$	h (ft)	$\frac{h}{\lambda}$	ν (deg)	Δz (ft)	$\frac{\Delta z}{h}$	$\frac{\omega_e}{\omega n(z)}$	$\Delta\tau$ (deg)	$\frac{\Delta\tau}{\nu^2}$	$\frac{\omega_e}{\omega n\phi}$	$\Delta\phi$ (deg)	$\frac{\Delta\phi}{\nu^2}$
C_Δ = 4.7																				
0	0.726	1.84	0.507	7.07	0.260	0.740	0.537	9.69	1.94	0.220	.0227	7.9	0.20	0.91	0.233	7.1	0.90	0.479	1.7	0.22
"	.722	0	0	7.11	0	1	0.722	9.81	1.96	0.228	.0232	8.0	0.17	0.75	0.314	6.5	0.81	0.645	2.3	0.29
"	.766	0	0	6.70	0	1	0.766	8.70	1.74	0.268	.0308	10.8	0.20	0.75	0.333	7.4	0.69	0.684	2.4	0.22
"	.769	1.84	0.507	6.68	0.276	0.724	0.556	8.64	1.73	0.257	.0298	10.4	0.16	0.62	0.242	6.7	0.65	0.496	2.3	0.22
"	1.106	0	0	4.65	0	1	1.106	4.18	0.84	0.291	.0697	24.3	0.04	0.14	0.481	4.6	0.18	0.988	1.2	0.05
"	1.106	1.84	0.507	4.65	0.396	0.604	0.668	4.18	0.84	0.285	.0682	23.8	0.01	0.04	0.290	3.5	0.15	0.596	5.2	0.22
135	0.724	0	0	7.08	0	1	0.724	9.75	1.95	0.224	.0230	8.0	0.19	0.85	0.315	6.1	0.76	0.646	9.9	1.24
"	.726	1.84	0.507	7.08	-0.184	1.184	0.861	9.69	1.94	0.220	.0227	7.9	0.20	0.91	0.374	6.0	0.76	0.769	7.7	0.98
"	.766	0	0	6.70	0	1	0.766	8.70	1.74	0.257	.0296	10.2	0.19	0.74	0.333	6.9	0.68	0.684	7.8	0.77
"	.763	1.84	0.507	6.70	-0.194	1.194	0.912	8.78	1.76	0.258	.0294	10.1	0.21	0.82	0.397	7.5	0.74	0.814	5.9	0.59
"	1.106	0	0	4.70	0	1	1.106	4.18	0.84	0.299	.0715	25.0	0.11	0.37	0.481	7.0	0.28	0.988	6.8	0.27
"	1.106	1.84	0.507	4.70	-0.277	1.277	1.410	4.18	0.84	0.298	.0713	24.9	0.10	0.34	0.613	6.6	0.27	1.259	5.9	0.24
45	1.106	0	0	4.70	0	1	1.106	4.18	0.84	0.318	.0761	26.5	0.12	0.38	0.481	6.5	0.25	0.988	9.5	0.36
"	1.106	1.84	0.507	4.70	0.277	0.723	0.799	4.18	0.84	0.318	.0761	26.5	0.05	0.16	0.347	6.6	0.25	0.713	9.7	0.37
"	0.769	0	0	6.68	0	1	0.769	8.64	1.73	0.253	.0293	10.2	0.19	0.75	0.334	7.0	0.69	0.687	11.0	1.08
"	0.769	1.84	0.507	6.68	0.195	0.805	0.618	8.64	1.73	0.262	.0304	10.5	0.15	0.57	0.269	5.5	0.53	0.552	9.9	0.95
"	0.726	0	0	7.07	0	0	0.726	9.69	1.94	0.219	.0226	7.9	0.17	0.78	0.316	6.6	0.84	0.648	14.3	1.81
"	0.726	1.84	0.507	7.07	0.184	0.816	0.592	9.69	1.94	0.221	.0228	8.0	0.17	0.75	0.257	5.1	0.64	0.529	9.4	1.18
90	1.106	0	0	4.70	0	1	1.106	4.18	0.84	0.364	.0870	30.3	0.27	0.74	0.481	0.5	0.17	0.988	7.5	0.25
"	1.106	1.84	0.507	4.70	0	1	1.106	4.18	0.84	0.353	.0845	29.5	0.20	0.57	0.481	0.1	0.03	0.988	9.5	0.32
"	0.766	0	0	6.70	0	1	0.766	8.70	1.74	0.261	.0300	10.4	0.19	0.14	0.333	2.0	0.19	0.684	9.6	0.92
"	0.763	1.84	0.507	6.73	0	1	0.763	8.78	1.76	0.252	.0287	10.0	0.24	0.95	0.332	1.8	0.18	0.681	6.9	0.69
"	0.726	0	0	7.07	0	1	0.726	9.69	1.94	0.278	.0287	10.0	0.28	1.01	0.316	1.7	0.17	0.648	8.0	0.80
"	0.724	1.84	0.507	7.09	0	1	0.724	9.75	1.95	0.271	.0278	9.6	0.27	1.00	0.315	1.7	0.18	0.646	11.0	1.15

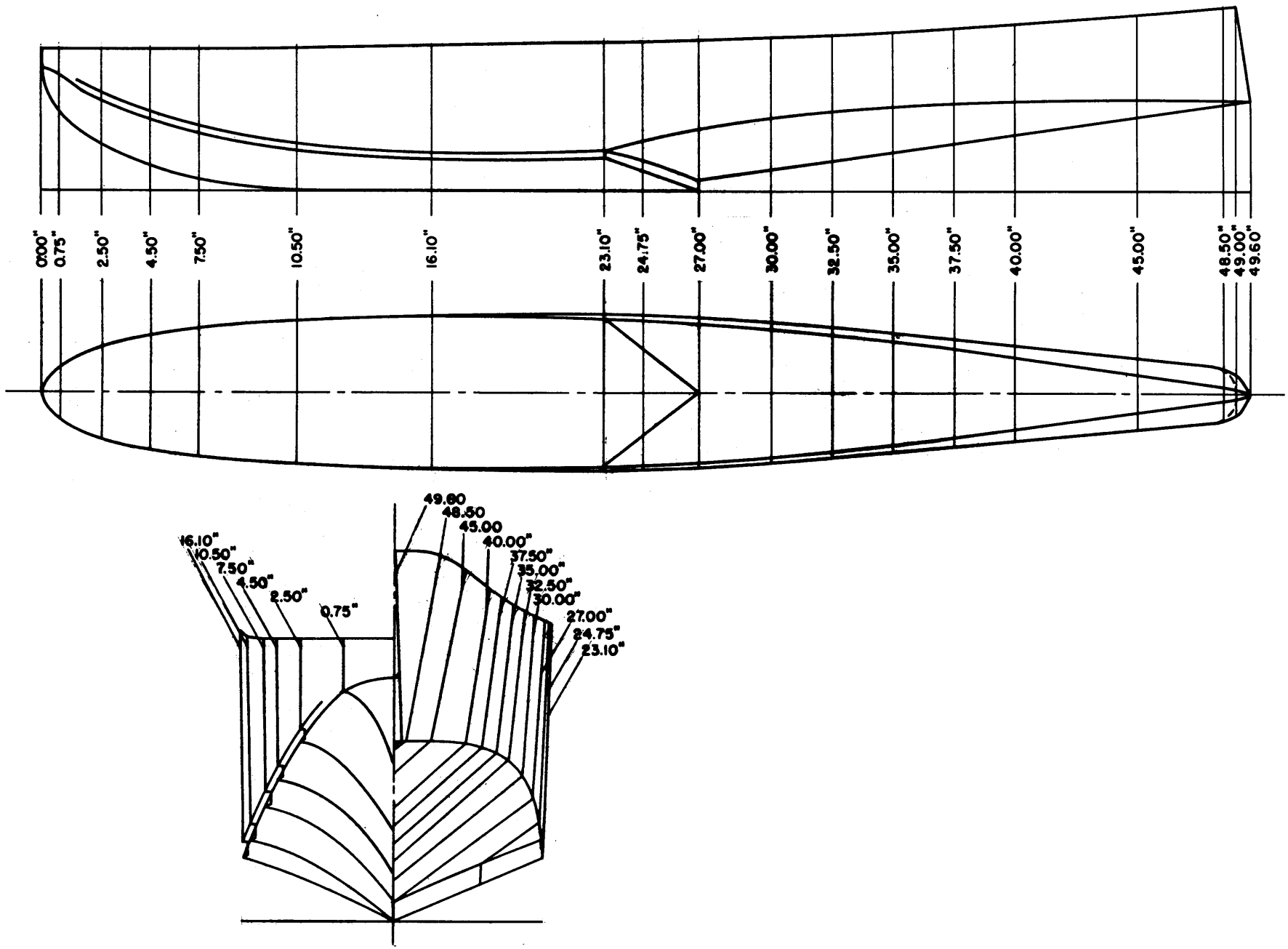

FIG. 1 HULL LINES FOR L/b=8 MODEL

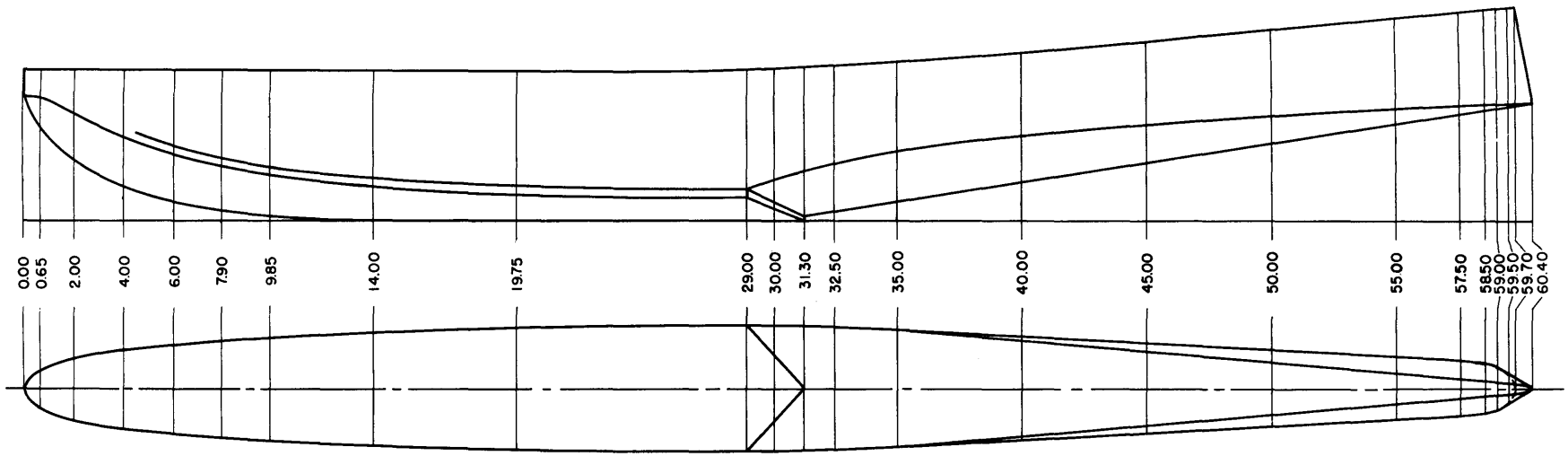

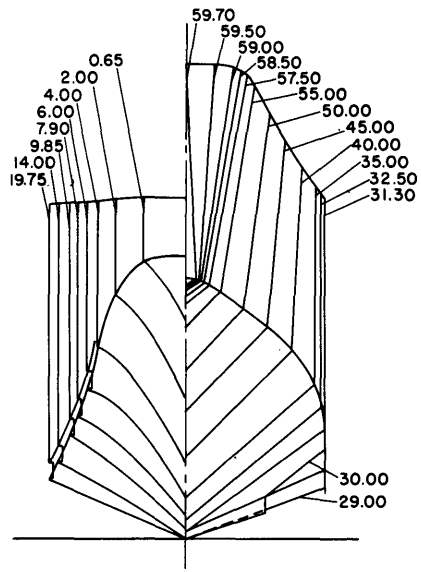

FIG. 2 HULL LINES FOR L/b=12 MODEL

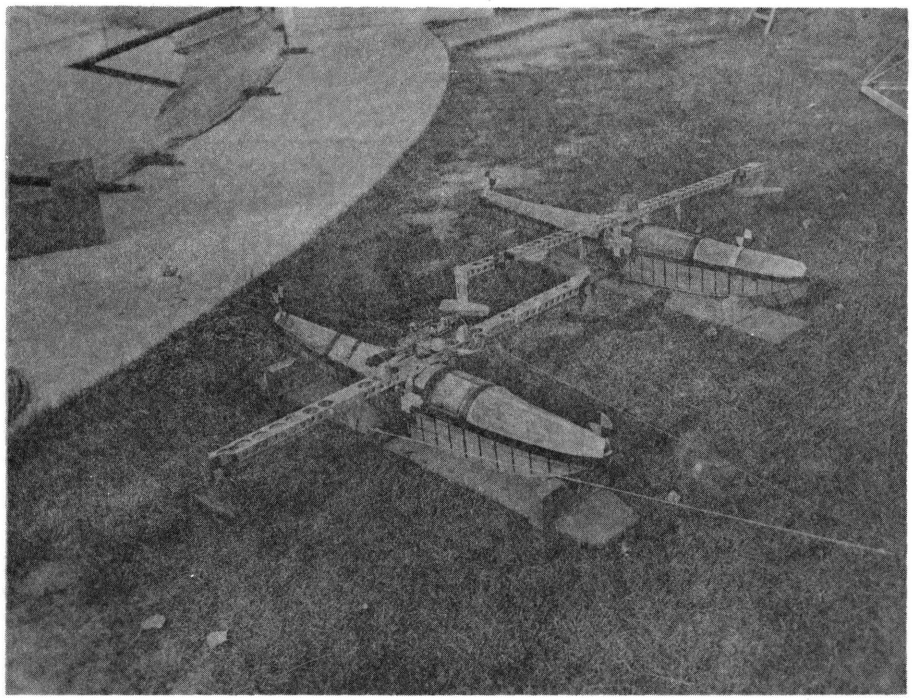

FIG. 3 PHOTOGRAPH OF MODEL HULLS IN TESTING CONFIGURATION

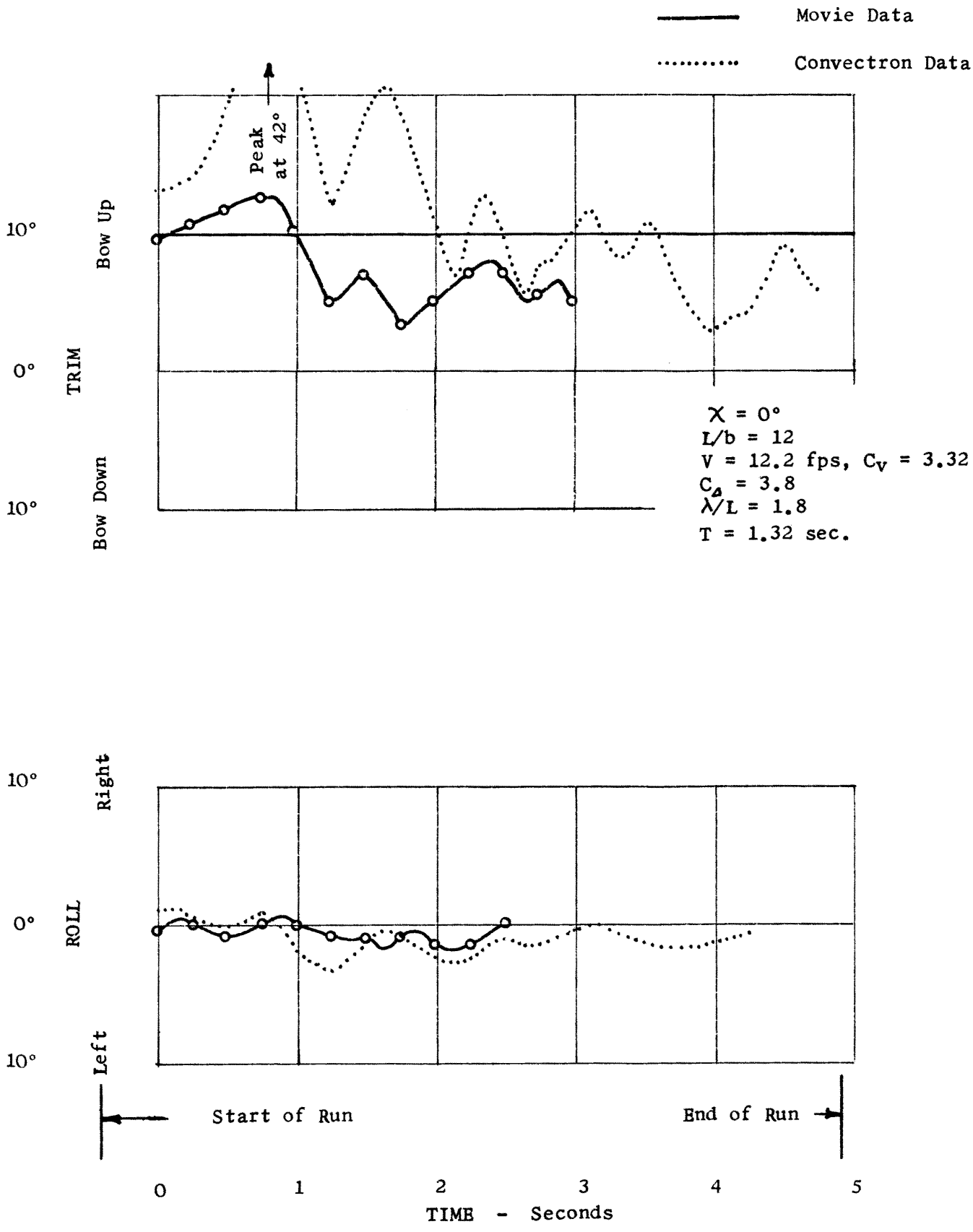

Fig. 4 COMPARISON OF CONVECTRON AND MOVIE DATA, $\chi = 0°$

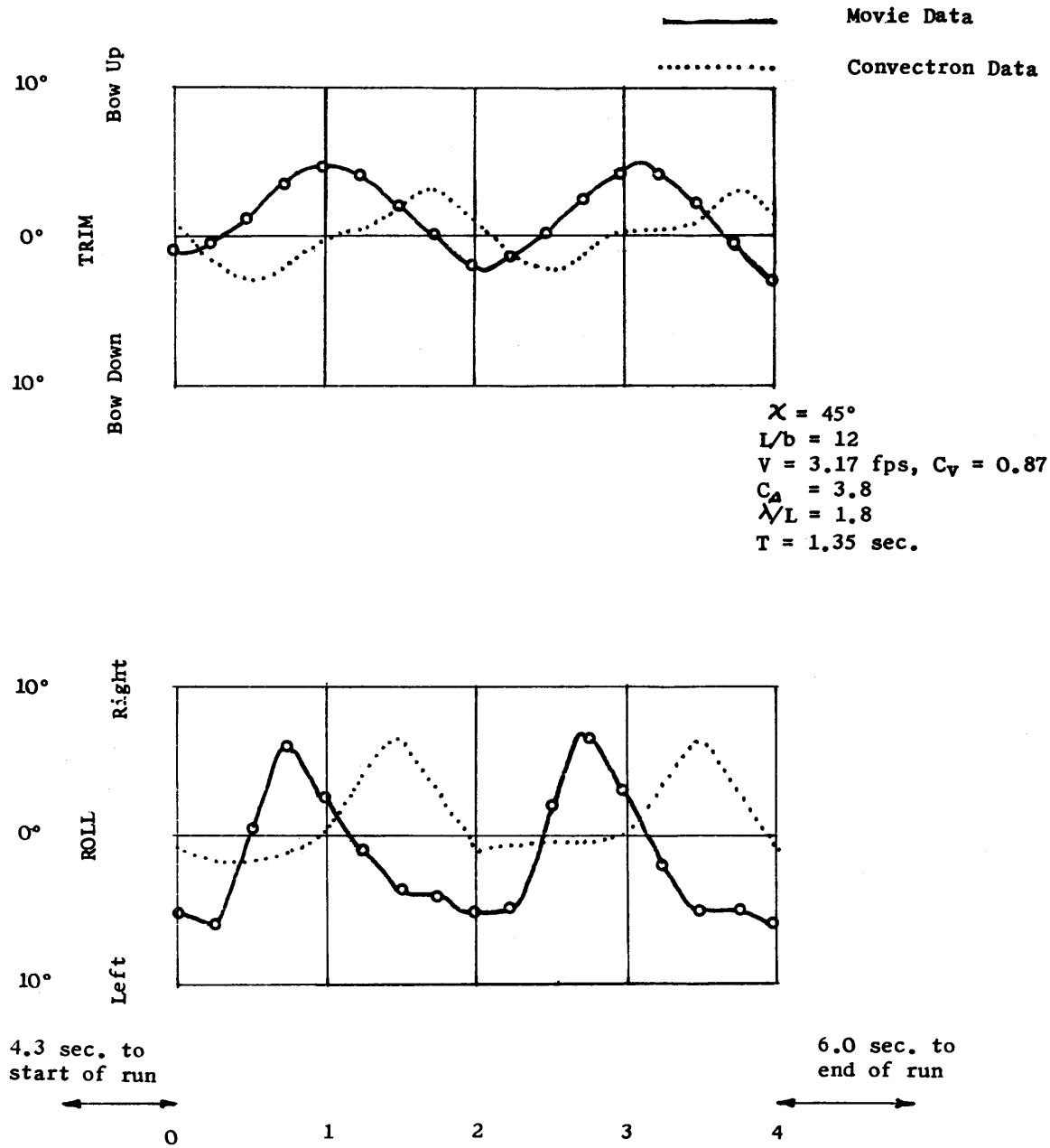

Fig. 5 COMPARISON OF CONVECTRON AND MOVIE DATA, $\chi = 45°$

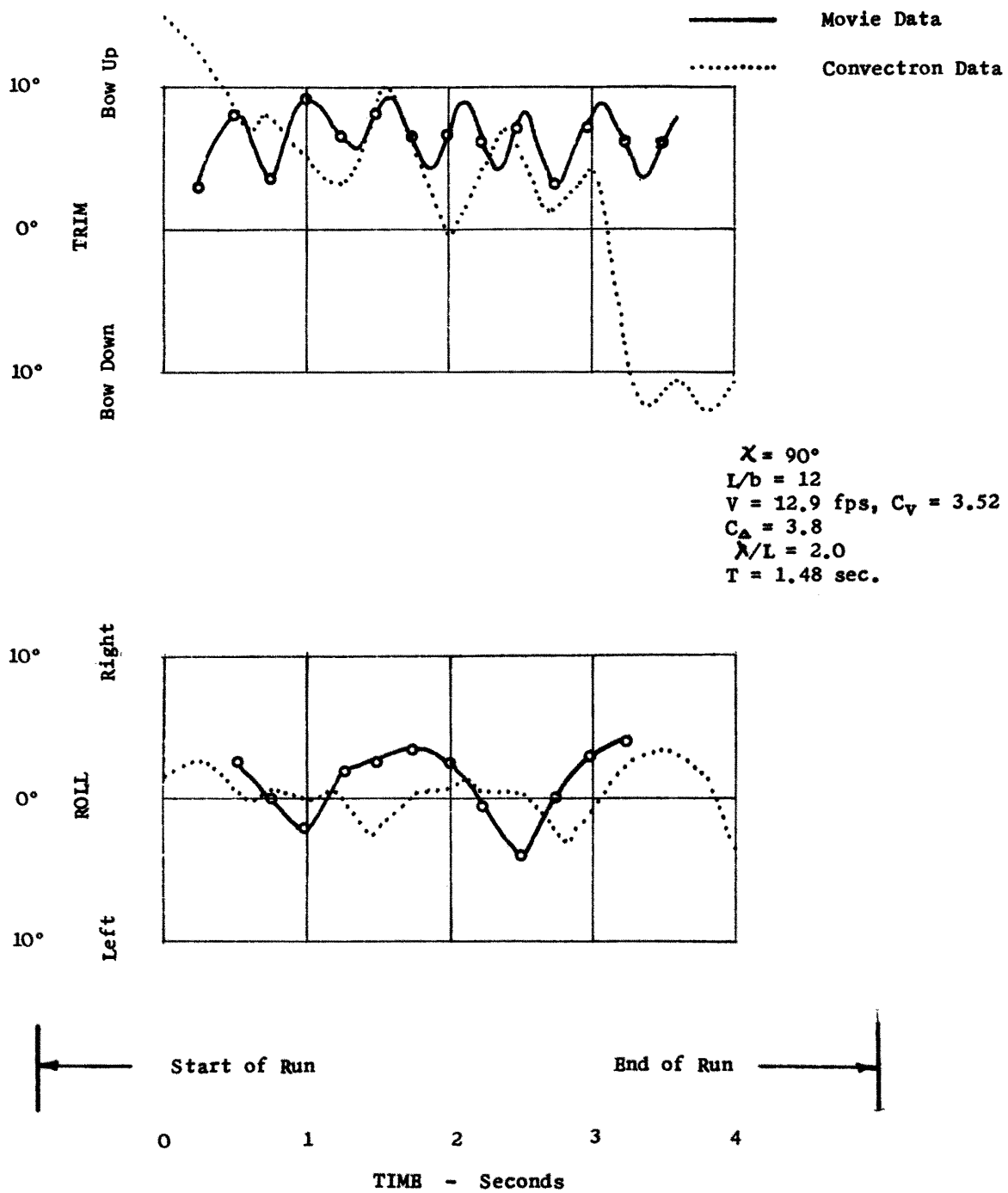

Fig. 6 COMPARISON OF CONVECTRON AND MOVIE DATA, $\chi = 90°$

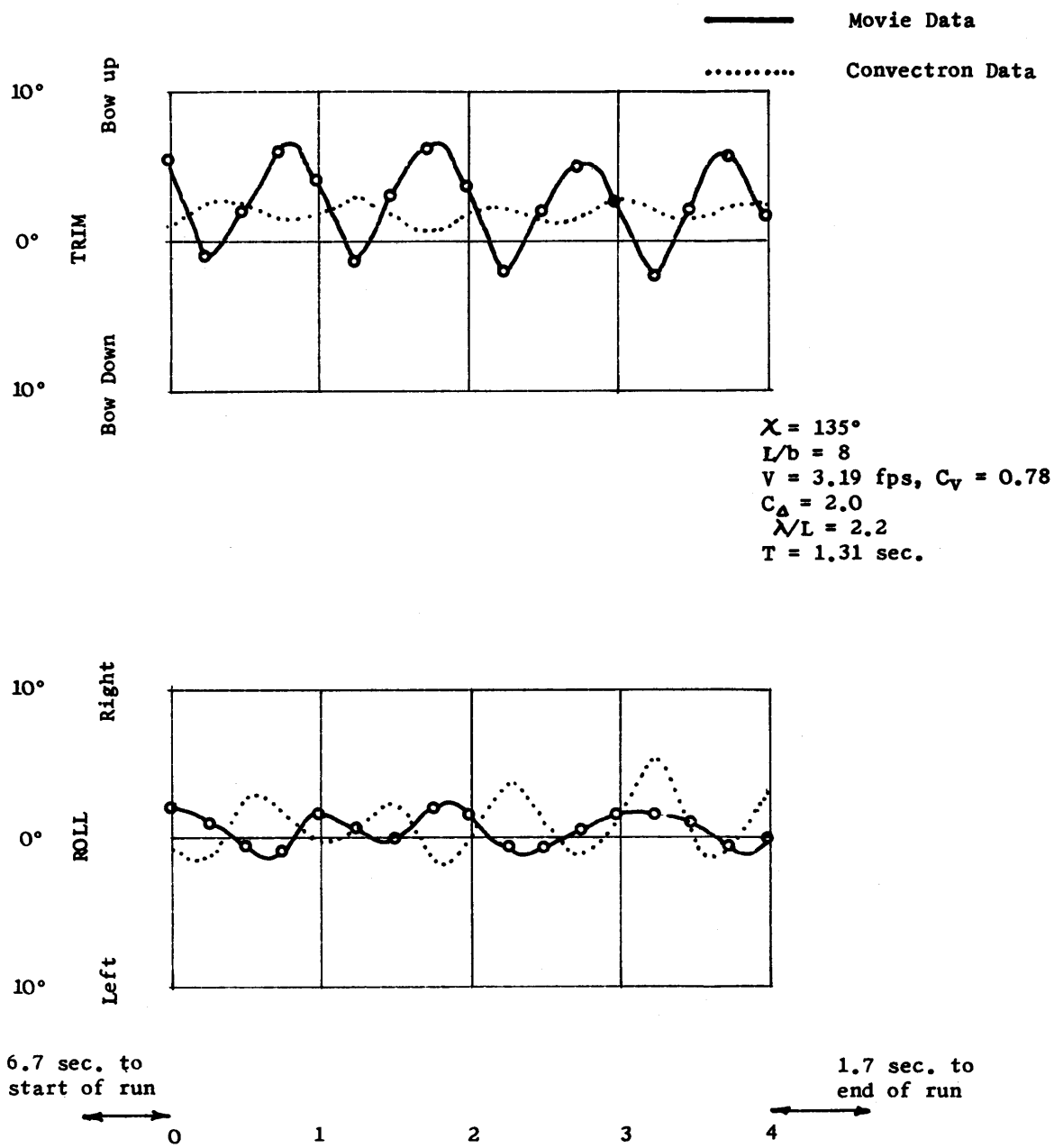

Fig. 7 COMPARISON OF CONVECTRON AND MOVIE DATA, χ = 135°

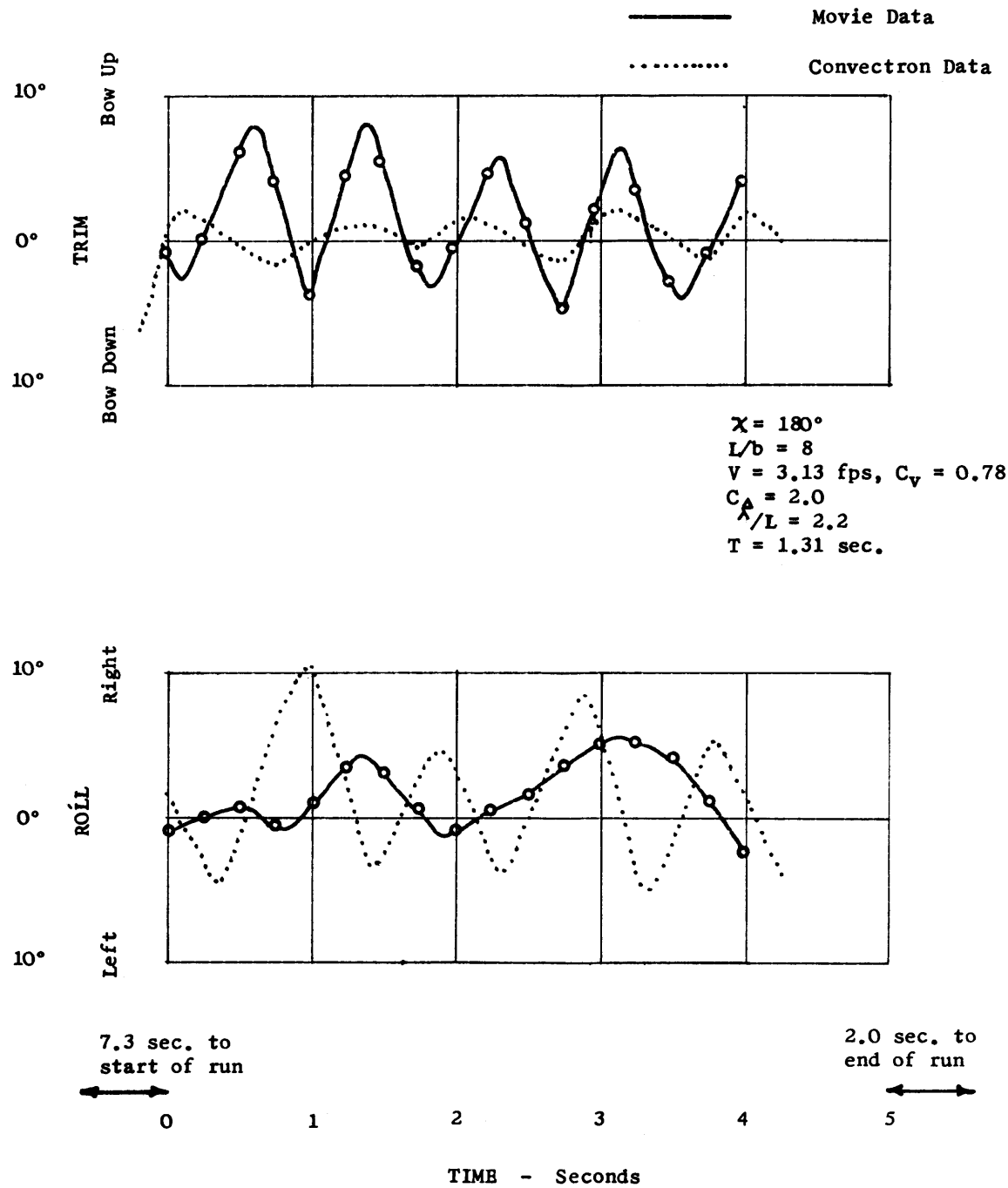

Fig. 8 COMPARISON OF CONVECTRON AND MOVIE DATA, χ = 180°

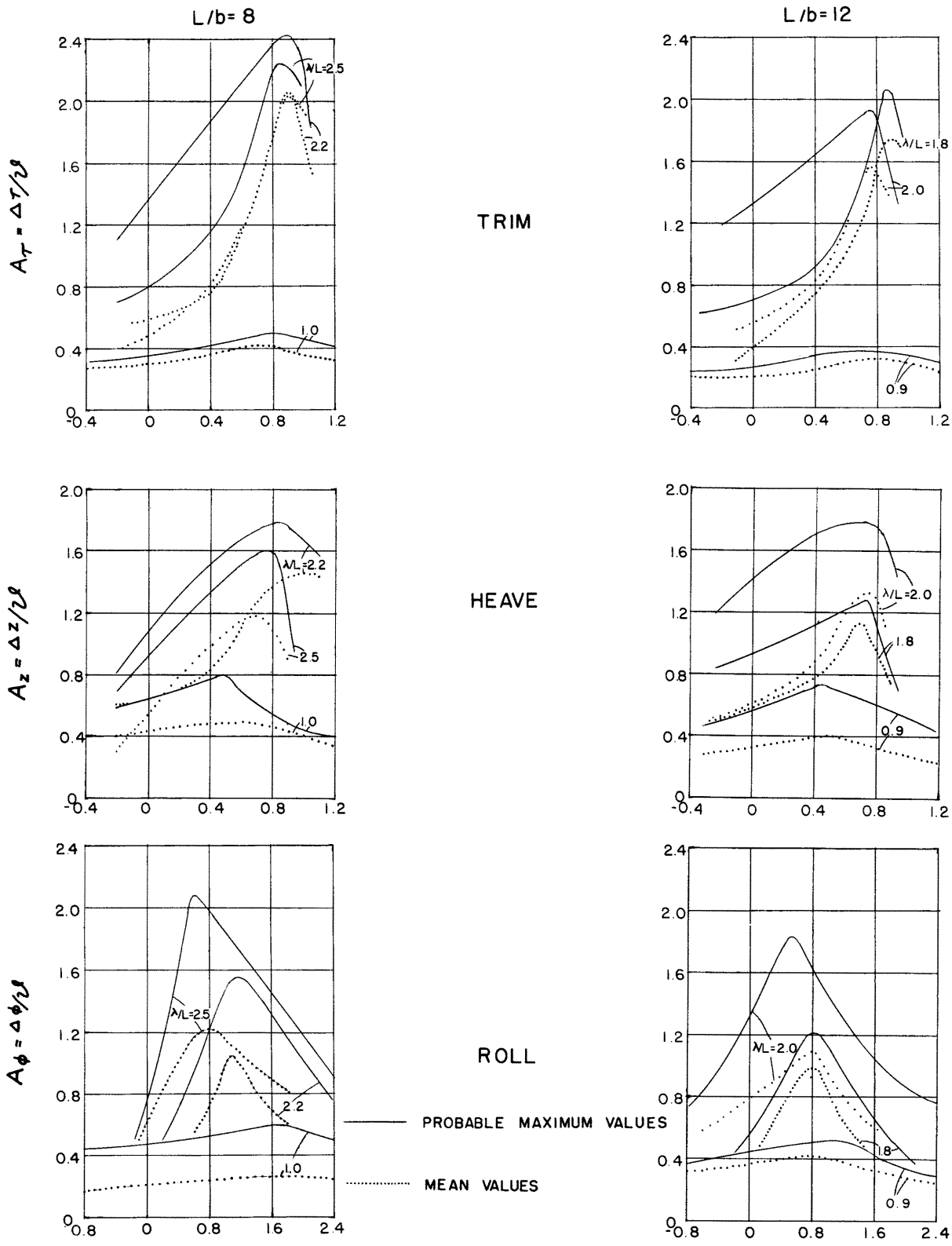

Fig. 9 AMPLITUDE PARAMETER AS A FUNCTION OF TUNING RATIO

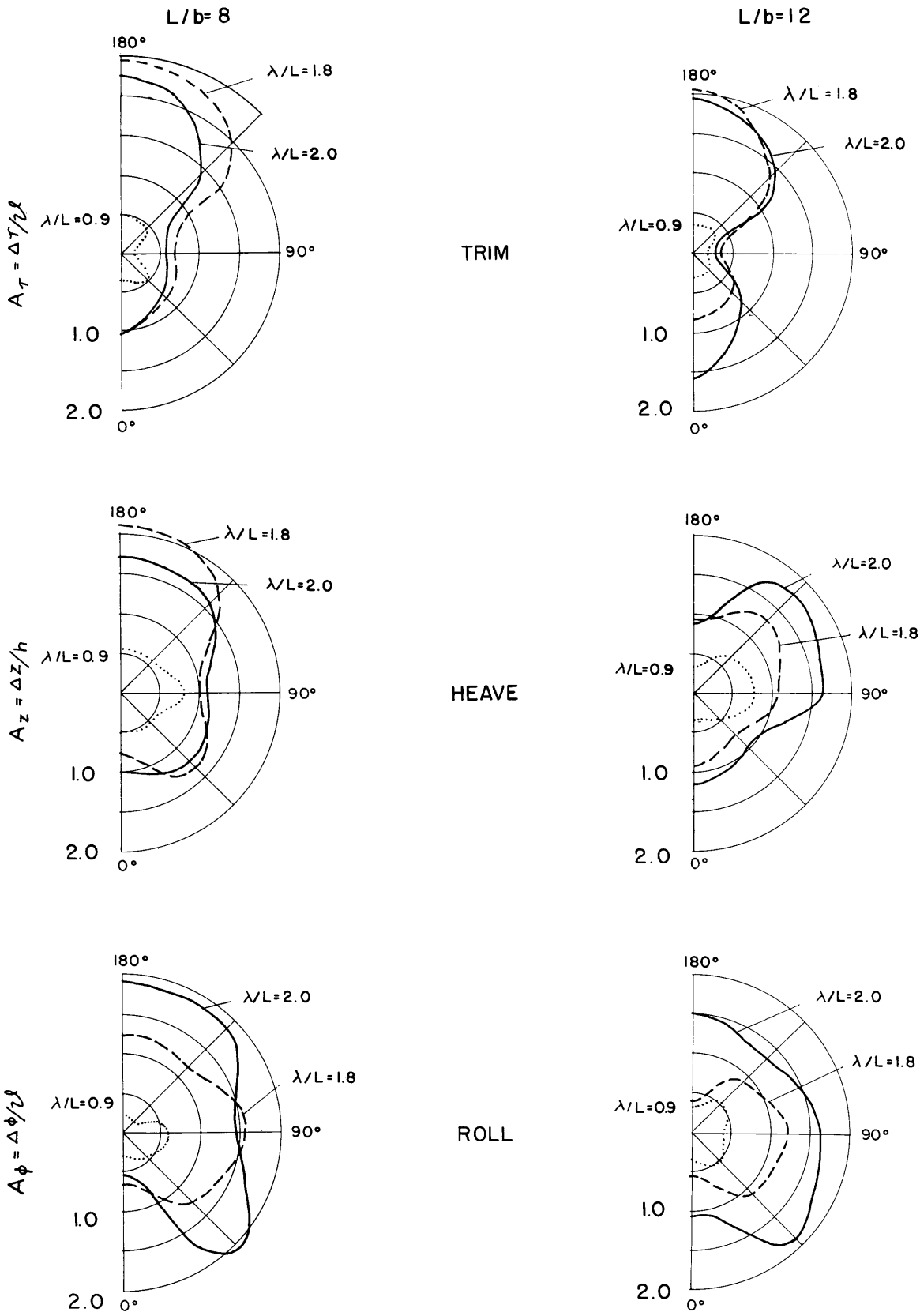

Fig. 10 AMPLITUDE PARAMETER AS A FUNCTION OF HEADING

L/b=8

L/b=12

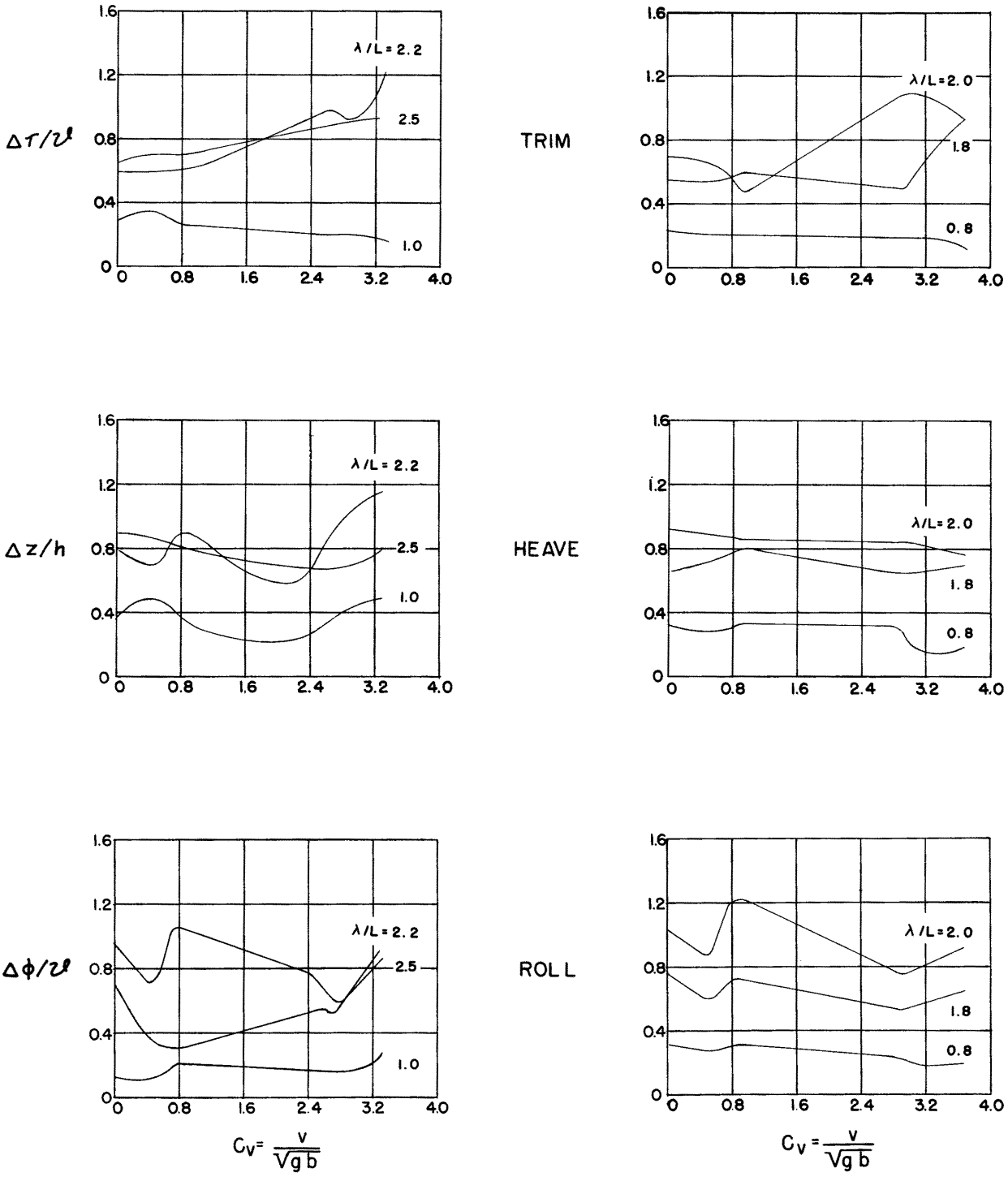

Fig. 11 AMPLITUDE PARAMETER AS A FUNCTION OF SPEED

$C_V = 0$

$C_V = 3.3$ or 3.7

$\Delta\tau/2\ell$

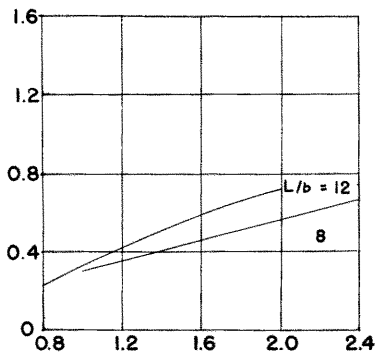

TRIM

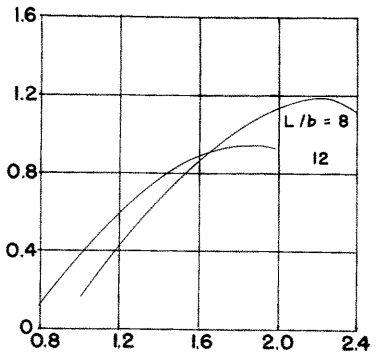

$\Delta z/h$

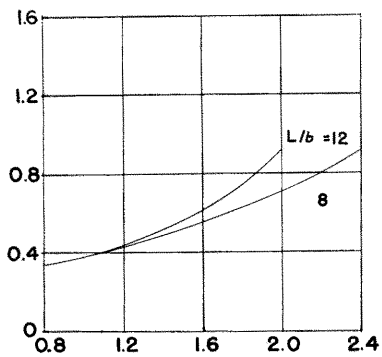

HEAVE

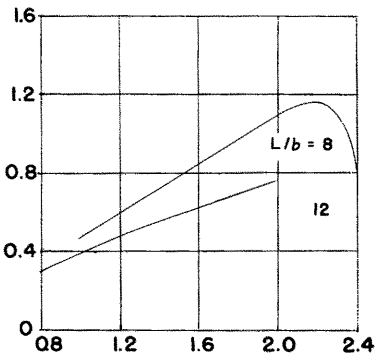

$\Delta\phi/2\ell$

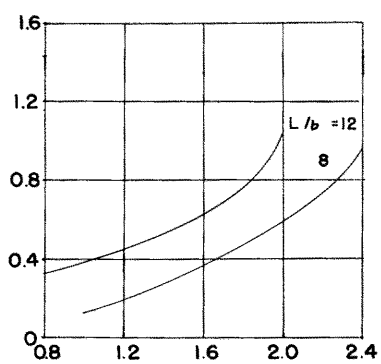

ROLL

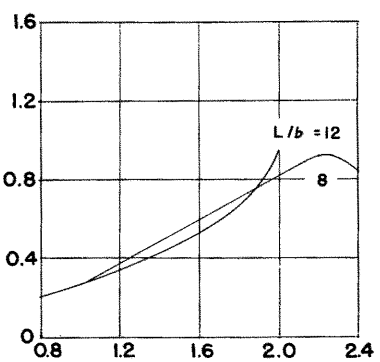

Fig. 12 AMPLITUDE PARAMETER AS A FUNCTION OF RELATIVE WAVE LENGTH